12-23 July 2021

Berlin, Germany

37th International Cosmic Ray Conference

Combined fit of the energy spectrum and mass composition across the ankle with the data measured at the Pierre Auger Observatory

Eleonora Guido (1,2)

on behalf of the Pierre Auger (3) Collaboration

(1) INFN Sezione Torino, Torino, Italy

(2) Università degli Studi di Torino, Torino, Italy

(3) Observatorio Pierre Auger, Av. San Martin Norte 304, 5613 Malargüe, Argentina

Introduction to the combined fit

CRs ejected by generic EG accelerators

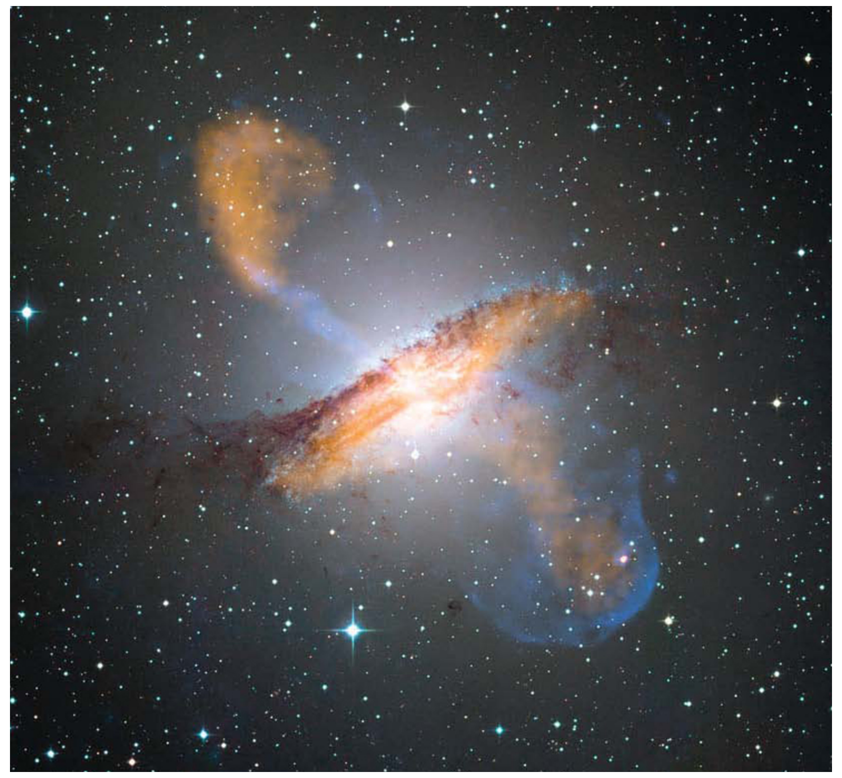

Assumptions on a simple astrophysical model

(CRs considered **at the escape**)

Propagation through the intergalactic medium

SimProp simulations

Choice of propagation models for uncertain quantities

+

Production of showers in the atmosphere

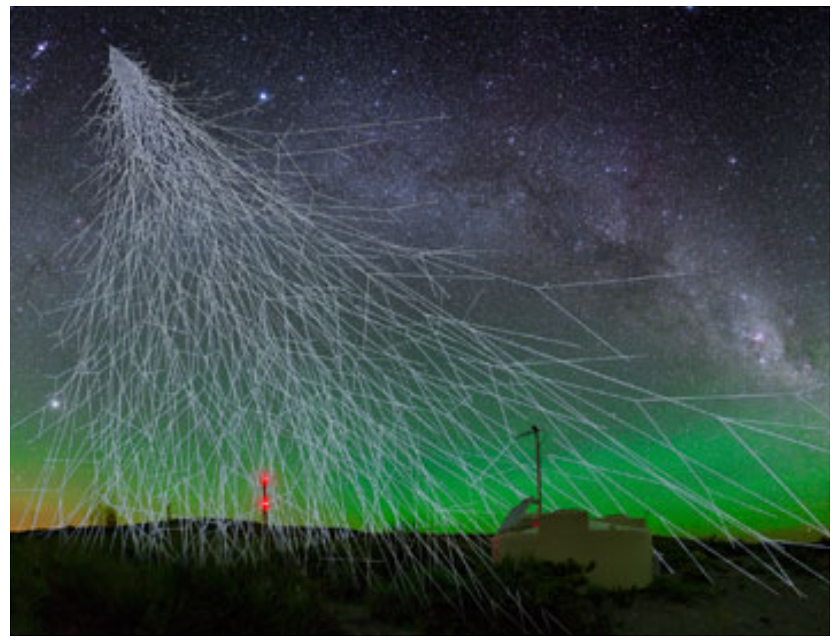

Choice of hadronic interaction models

Comparison with the data (detector effects are included)

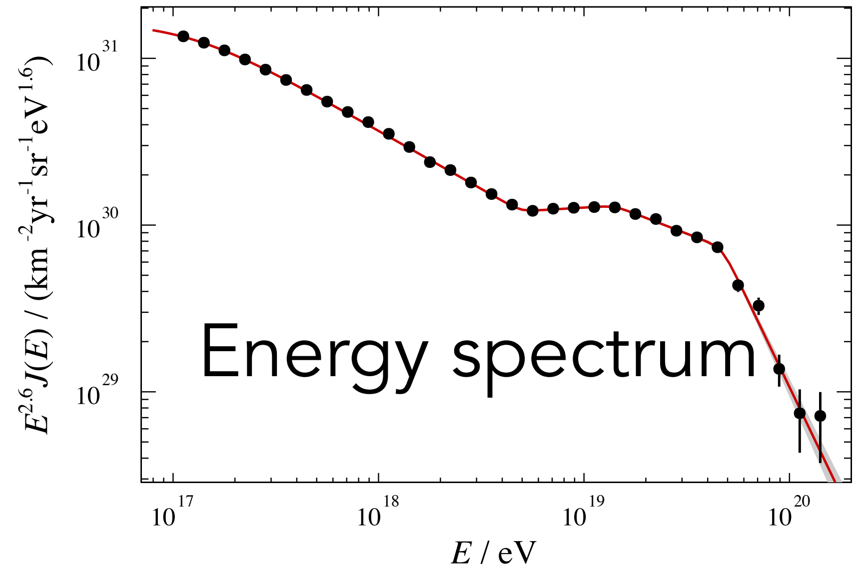

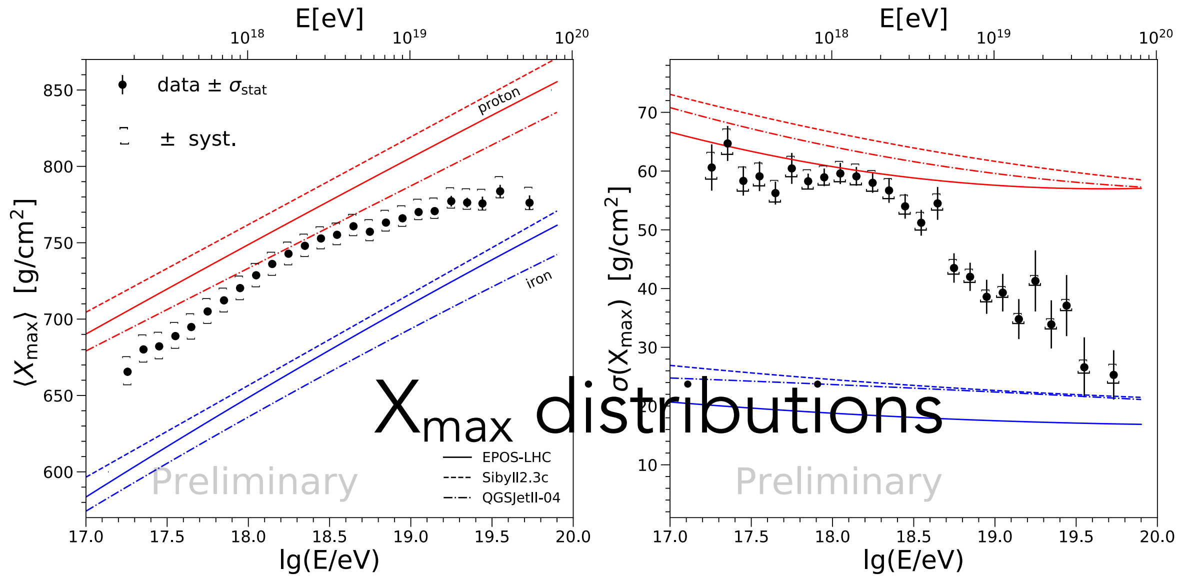

- Description of the Auger measurements in the ankle region with the superposition of different Galactic/extragalactic contributions
- Inference about ***the physical parameters related to the energy spectrum and the mass composition of particles escaping the environments of EG sources***
- Impact on the results of the **systematic uncertainties**
- Effect of the **assumptions on the source evolution** on the fit results

The astrophysical model

Generic population of extragalactic sources

- population of identical sources
- uniform distribution except for a local overdensity for $d < 30$ Mpc
- ejection of n representative nuclear species A, chosen among ^{1}H, ^{4}He, ^{14}N, ^{28}Si, ^{56}Fe

Energy spectrum escaping from the source environment

$$J(E) = \sum_A f_A \cdot J_0 \cdot \left(\frac{E}{E_0}\right)^{-\gamma} \cdot \begin{cases} 1, & E < Z_A \cdot R_{\text{cut}}; \\ \exp\left(1 - \frac{E}{Z_A \cdot R_{\text{cut}}}\right), & E > Z_A \cdot R_{\text{cut}}. \end{cases}$$

Characterising the escape spectrum → parameters estimated in the fit

- Spectral parameters γ , R_{cut}

- Energy spectrum normalisation J_0

$$J_0 \longrightarrow \mathscr{L}_0 = \frac{4\pi}{d_{\max}} \sum_{\text{A}} \int_{E_{\min}}^{\infty} E\, J_A(E)\, dE$$

expressed in $\text{erg} \cdot \text{Mpc}^{-3} \cdot \text{yr}^{-1}$

Emissivity of a population: total energy ejected per unit of comoving volume and time

- Mass fractions f_A at the energy E_0

$$f_A \longrightarrow I_A = \frac{\int_{E_{\min}}^{\infty} J_A(E) E dE}{\sum_A \int_{E_{\min}}^{\infty} J_A(E) E dE}$$

Fractions of the integral of the energy density above $E_{min} = 10^{17}$ eV

The astrophysical model

Generic population of extragalactic sources

- population of identical sources
- uniform distribution except for a local overdensity for $d < 30$ Mpc
- ejection of n representative nuclear species A, chosen among ^{1}H, ^{4}He, ^{14}N, ^{28}Si, ^{56}Fe

Energy spectrum escaping from the source environment

$$J(E) = \sum_A f_A \cdot J_0 \cdot \left(\frac{E}{E_0}\right)^{-\gamma} \cdot \begin{cases} 1, & E < Z_A \cdot R_{\rm cut}; \\ \exp\left(1 - \frac{E}{Z_A \cdot R_{\rm cut}}\right), & E > Z_A \cdot R_{\rm cut}\,. \end{cases}$$

Propagation through the IGM and the Earth's atmosphere

- SimProp simulations for the propagation in the IGM → **model for the photo-disintegration cross sections $\sigma_{\rm pd}$**
  → **model for the EBL spectrum and evolution**

- Different possible **hadronic interaction models** for the propagation in the atmosphere

$\sigma_{\rm pd}$	**T**alys, **P**SB
EBL	**G**ilmore, **D**ominguez
HIM	**E**POS-LHC, **S**ibyll2.3d, **Q**GSJetIIv4

← PSB (*Puget, Stecker and Bredekamp (1976)*)
TALYS *(Koning, Hilaire and Duijvestijn (2005))*

***Gilmore** et al. (2012)*
***Dominguez** et al. (2011)*

← *post-LHC hadronic interaction models*

Data set and fit procedure

Data in $\log_{10}(E/eV)$ bins of 0.1 width fitted above $E \sim 6\ 10^{17}$ eV

- We aim at interpreting the ankle region
- At lower energy the Galactic CRs would be become dominant

} We use only the **data from the standard fluorescence telescopes** for the X_{max} distributions ($\log_{10}(E/eV) > 17.8$)

→ in the future the the threshold could be lowered to ~10^{17} eV thanks to data from HEAT (High Elevation Auger Telescopes)

Data sets:

- Energy spectrum: last bin at $10^{20.2}$ eV [Pierre Auger Collaboration to be submitted to Eur. Phys. J. C.]
- X_{max} distributions: up to $10^{19.7}$ eV (+ 1 additional bin for events above), binned in intervals of X_{max} of 20 g cm^{-2} [A.Yushkov for the Pierre Auger Collaboration PoS(ICRC2019)482]

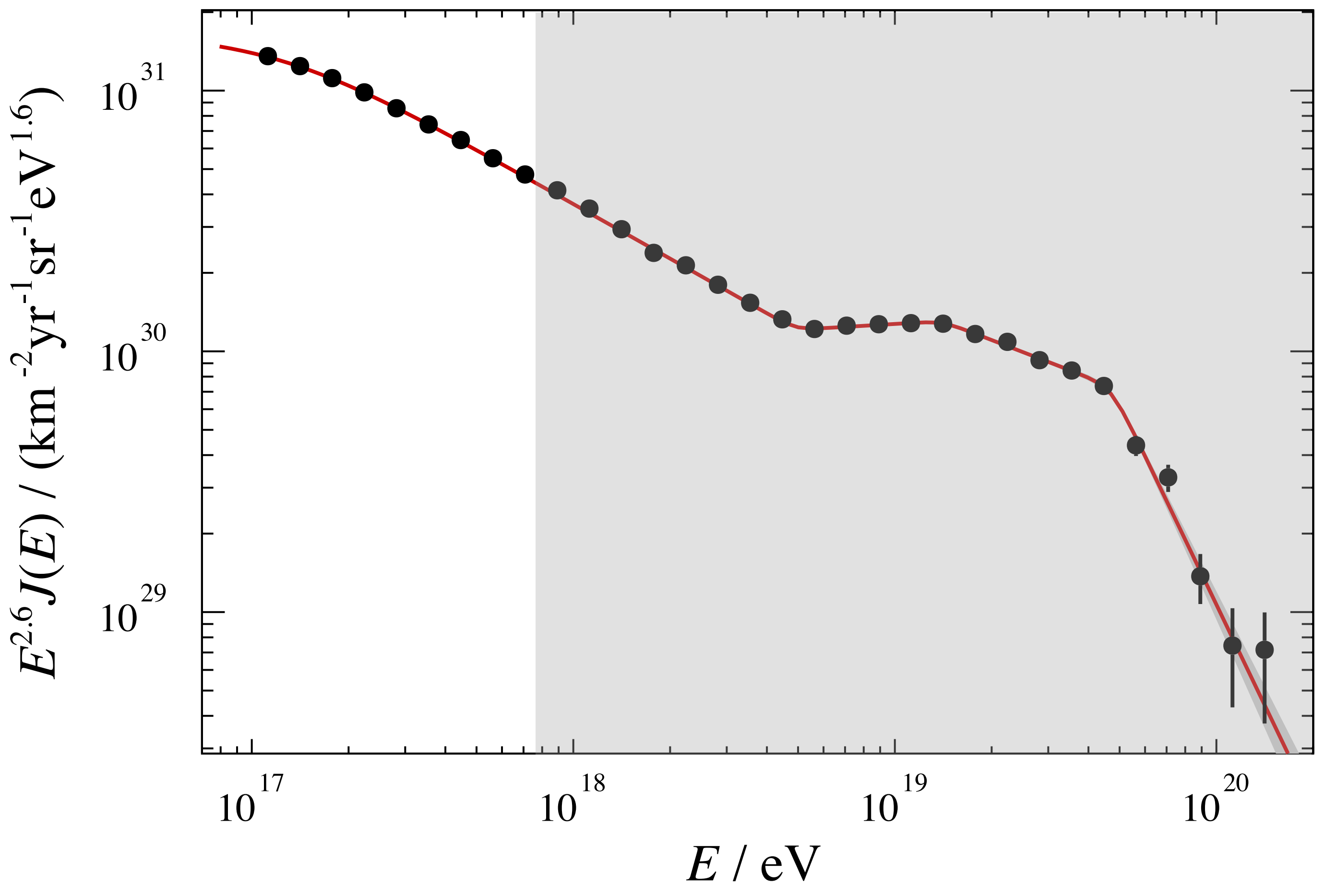

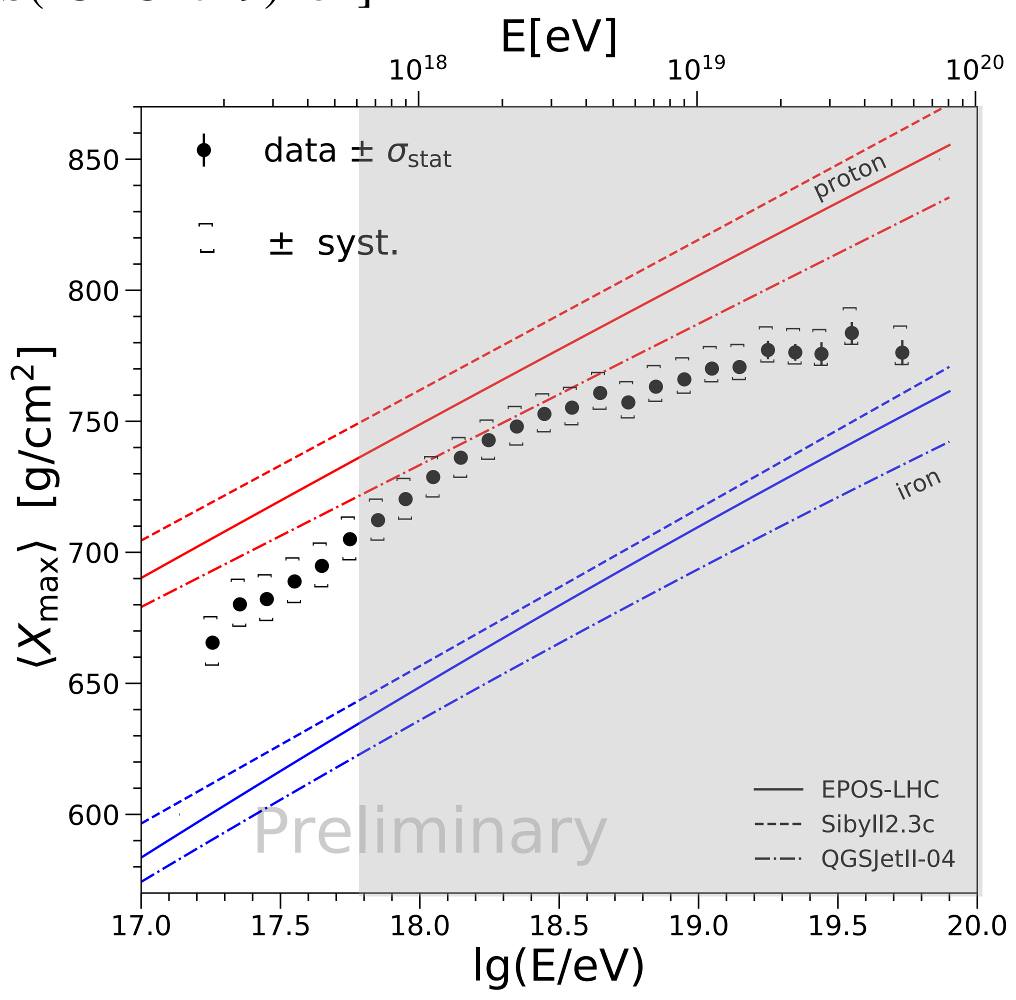

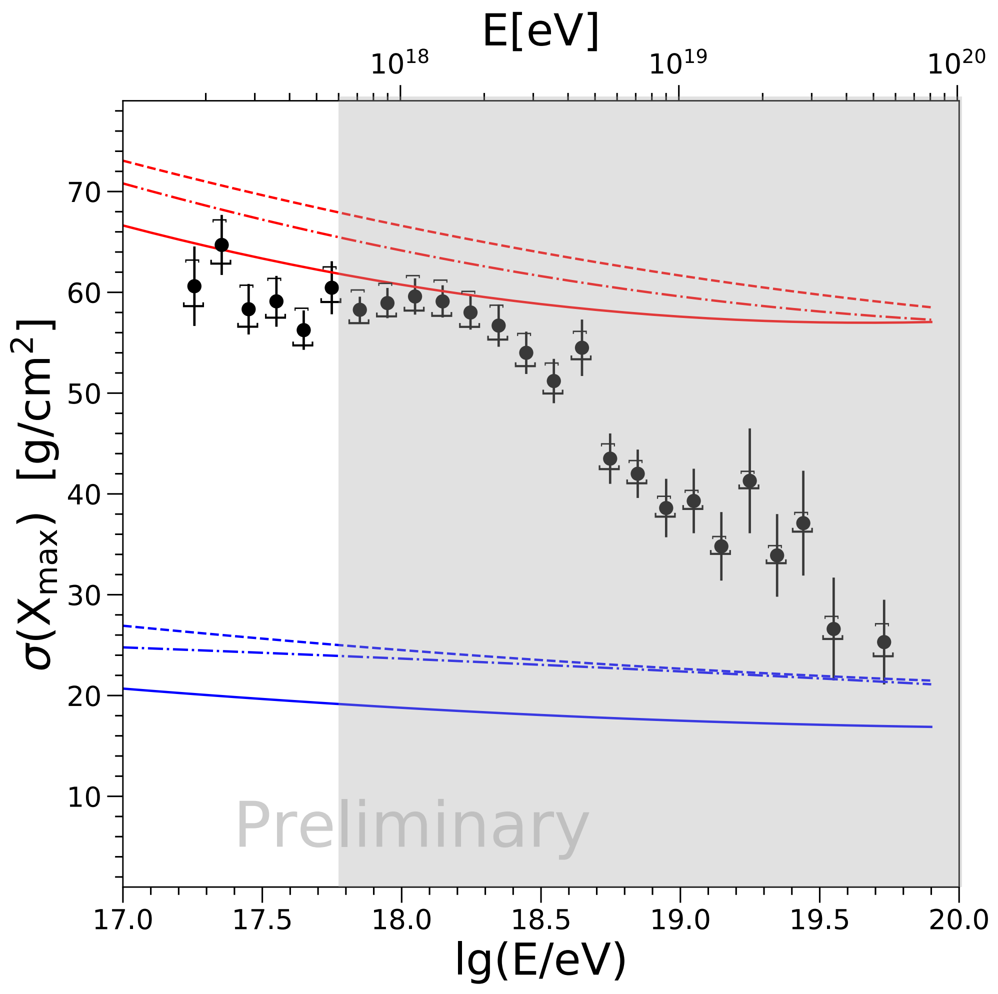

First two moments of the X_{max} distributions for figurative purposes

Data set and fit procedure

Data in $\log_{10}$(E/eV) bins of 0.1 width fitted above E ~ 6 10^{17} eV

- We aim at interpreting the ankle region
- At lower energy the Galactic CRs would be become dominant

We use only the **data from the standard fluorescence telescopes** for the X_{max} distributions ($\log_{10}$(E/eV) > 17.8)

The fit procedure:

The observed and simulated fluxes are compared by minimising the deviance D

$$D = D(J) + D(X_{\max}) = -2\ \ln\left(\frac{\mathscr{L}}{\mathscr{L}^{\rm sat}}\right) = -2\ \ln\left(\frac{\mathscr{L}_{\rm J}}{\mathscr{L}^{\rm sat}_{\rm J}}\right) - 2\ \ln\left(\frac{\mathscr{L}_{\rm X_{max}}}{\mathscr{L}^{\rm sat}_{\rm X_{max}}}\right)$$

- **Energy spectrum** → Gaussian distributions

$$L_{\rm J} = \prod_i \frac{1}{\sqrt{2\pi\sigma_i^2}} \exp\left(-\frac{(J_i^{\rm obs} - J_i^{\rm mod})^2}{2\sigma_i^2}\right),$$

observed unfolded flux
(detector effects)

expected simulated flux

- **X_{max} distributions** → multinomial distributions

$$L_{\rm X_{max}} = \sum_i n_i^{\rm obs}! \sum_j \frac{1}{k_{i,j}^{\rm obs}!} (G_{i,j}^{\rm mod})^{k_{i,j}^{\rm obs}}$$

i = $\log_{10}$(E) bin, j = X_{max} bin

observed events

model probability
(Gumbel distribution + detector effects)

The combined fit across the ankle

Simplest extension to lower energies of the above-ankle combined fit published in JCAP04(2017)038 → **fit above $10^{17.8}$ eV**

The astrophysical model: superposition of different contributions to describe the ankle feature and the energy region below it

- The ***above-ankle region*** is described by an EG component with a mixed (free) mass composition
- The ***region below the ankle*** is described by two scenarios:

A. *One additional EG component of protons + a heavier Galactic contribution at Earth*

- Interactions in the source sites could produce an *additional pure p component at lower energies with a softer energy spectrum*
- An additional heavier component is needed to describe the composition below the ankle
  - → Galactic contributions with a simple generic shape and different possible mass compositions (1/2 nuclear species)

Galactic contribution at Earth (no propagation):

single power law, with arbitrary spectral index + exponential cutoff

$$J(E) = \sum_{i=1}^{2} A_i J_0 \cdot \left(\frac{E}{E_0}\right)^{\gamma_g} \cdot \exp\left(-\frac{E}{R_{\text{cut}}}\right)$$

Fixed: $\gamma = -3.2$ (arbitrary value)

Fixed: $E_0 = 10^{16.85}$ eV

- Cutoff R_{cut}
- Normalisation J_0
- Fraction of A_1 and A_2 at $E_0 : f_{A1}, f_{A2}$ (if there are 2 species)

→ free parameters

The combined fit across the ankle

Simplest extension to lower energies of the above-ankle combined fit published in JCAP04(2017)038 → **fit above $10^{17.8}$ eV**

The astrophysical model: superposition of different contributions to describe the ankle feature and the energy region below it

- The ***above-ankle region*** is described by an EG component with mixed composition
- The ***region below the ankle*** is described by two scenarios:

    A. One additional EG component of protons + a heavier Galactic contribution at Earth

    - Interactions in the source sites could produce an *additional pure p component at lower energies with a softer energy spectrum*
    - An additional heavier component is needed to describe the composition below the ankle

      → Galactic contributions with a simple generic shape and different possible mass compositions (1/2 nuclear species)

    B. One additional mixed component ejected by EG sources

    - It could be ejected by another population of EG sources

      → similar to the one above the ankle but characterised by *different physical parameters* (spectral parameters, emissivity, mass composition)

Fit results in the two scenarios

Models configuration: Talys, Gilmore, EPOS-LHC

Scenario A

Gal. contribution +
EG component of pure p

Galactic contribution (at Earth)	N+Si	
J_0^{gal} [eV^{-1} km^{-2} sr^{-1} yr^{-1}]	$(1.07 \pm 0.06) \cdot 10^{-13}$	
$\log_{10}(R_{\mathrm{cut}}^{\mathrm{gal}}/\mathrm{V})$	17.48 ± 0.02	
f_{N} (%)	93.0	
EG components (at the sources)	**Low energy**	**High energy**
$\mathcal{L}_0$ [erg Mpc^{-3} yr^{-1}]	$7.28 \cdot 10^{45}$	$4.4 \cdot 10^{44}$
γ	3.30 ± 0.05	-1.47 ± 0.12
$\log_{10}(R_{\mathrm{cut}}/\mathrm{V})$	24 (lim.)	18.19 ± 0.02
I_{H} (%)	100 (fixed)	0.0
I_{He} (%)	-	27.17
I_{N} (%)	-	69.86
I_{Si} (%)	-	0.0
I_{Fe} (%)	-	2.97
D_J (N_J)	49.5 (24)	
$D_{X_{\max}}$ ($N_{X_{\max}}$)	593.8 (329)	
D (N)	643.3 (353)	

Scenario A

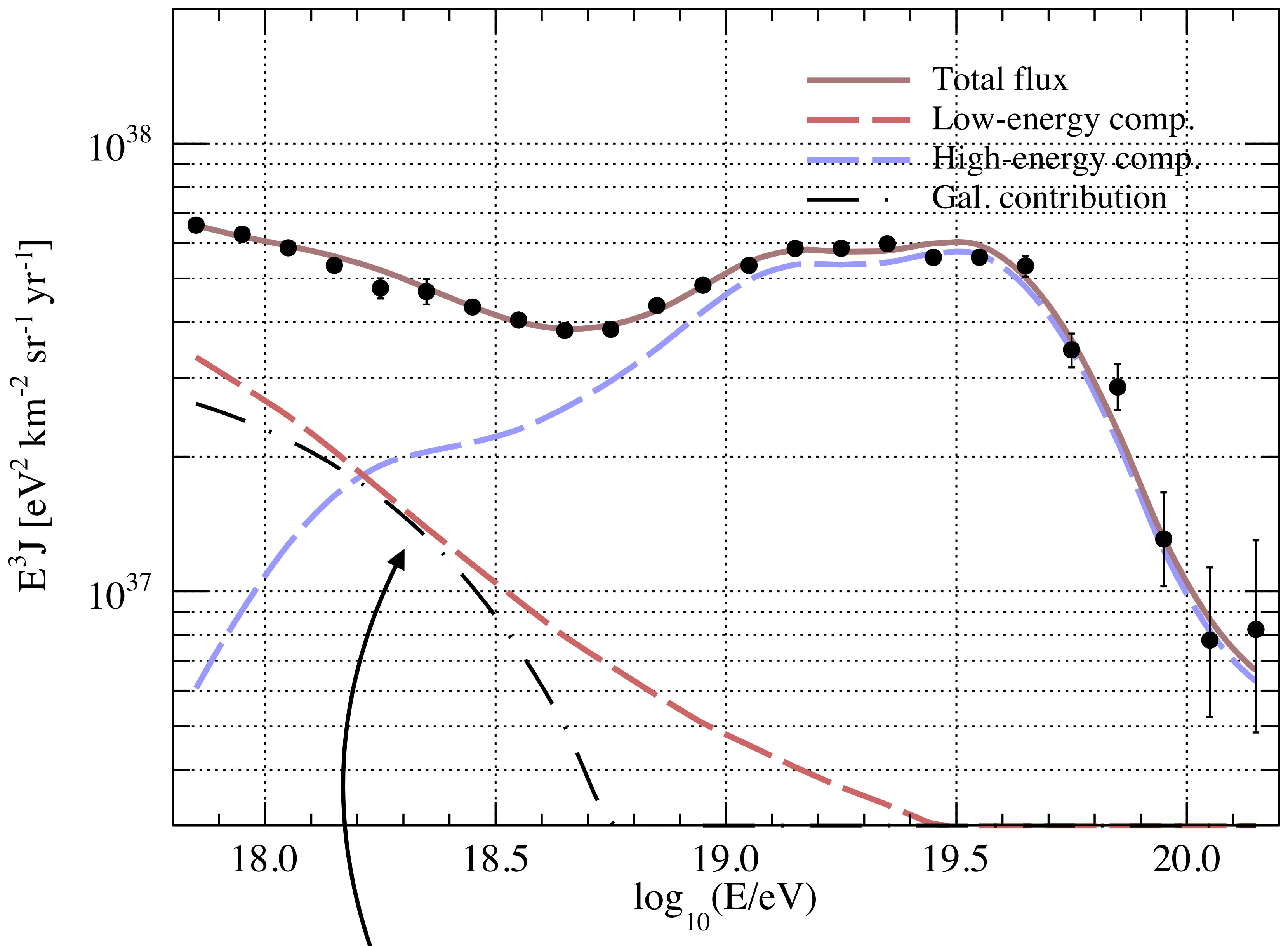

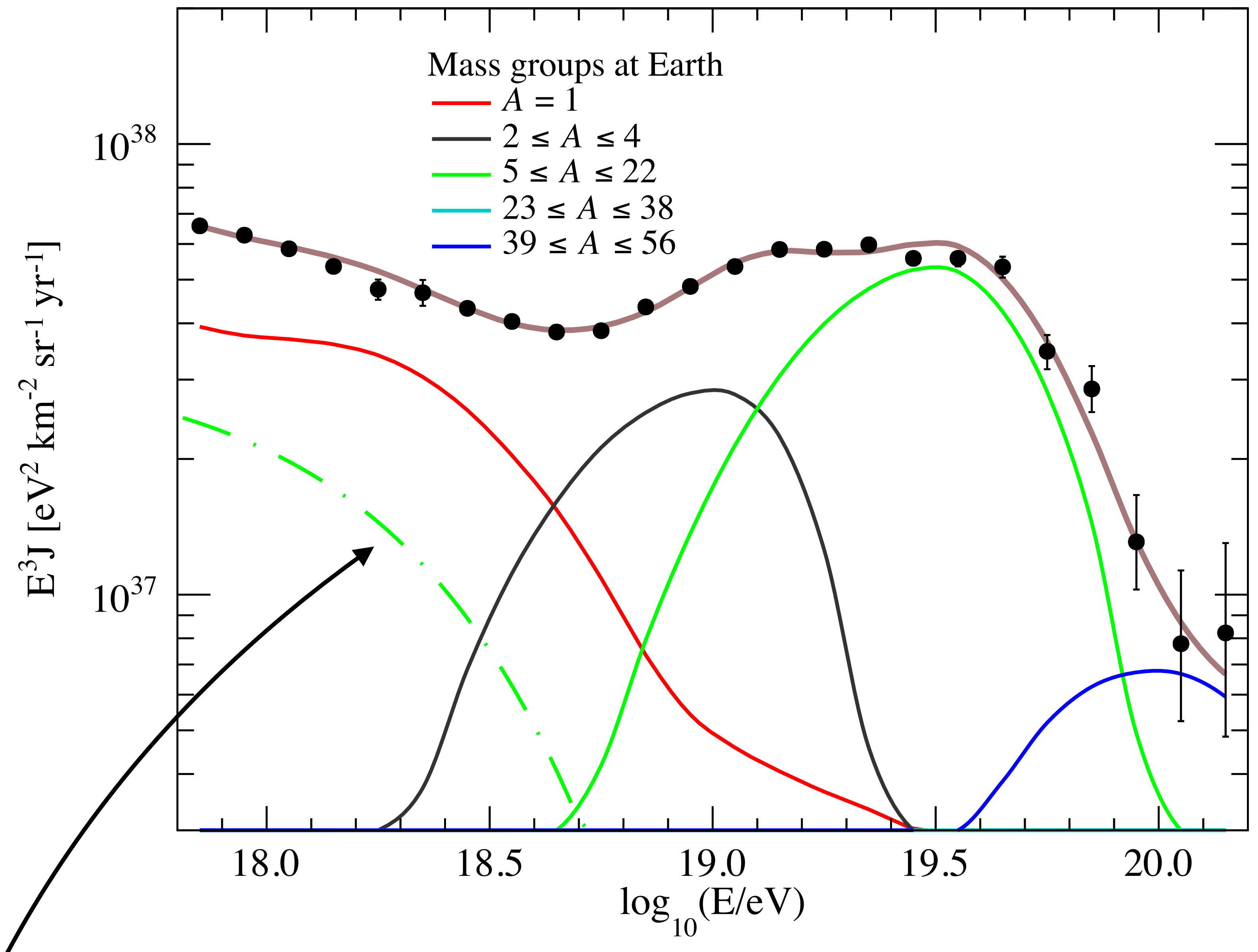

Galactic component:

- Additional contribution below the ankle if the LE component is of pure protons
- A contribution ***dominated by intermediate masses*** (e.g. N, as above) is favoured
- A heavier contribution (e.g. Si, Fe) is disfavoured (D ~ 1000)

- Extending up to ~ $4 \cdot 10^{18}$ eV
- Dominated by medium-mass nuclei

} At variance with SNRs standard model → only heavy nuclei up to ~10^{17} eV

→ possible explanation: additional Galactic component of CRs accelerated in Wolf-Rayet stars winds (N nuclei can be accelerated up to ~10^{18} eV)

[S. Thoudam et al., A&A Volume 595, A33, November 2016]

Fit results in the two scenarios

Models configuration: Talys, Gilmore, EPOS-LHC

	Scenario A: Gal. contribution + EG component of pure p		Scenario B: Two EG mixed components	
Galactic contribution (at Earth)	N+Si		-	
J_0^{gal} [eV^{-1} km^{-2} sr^{-1} yr^{-1}]	$(1.07 \pm 0.06) \cdot 10^{-13}$		-	
$\log_{10}(R_{cut}^{gal}/V)$	17.48 ± 0.02		-	
f_N (%)	93.0		-	
EG components (at the sources)	Low energy	High energy	Low energy	High energy
$\mathcal{L}_0$ [erg Mpc^{-3} yr^{-1}]	$7.28 \cdot 10^{45}$	$4.4 \cdot 10^{44}$	$1.7 \cdot 10^{46}$	$4.5 \cdot 10^{44}$
γ	3.30 ± 0.05	-1.47 ± 0.12	3.49 ± 0.02	-1.98 ± 0.10
$\log_{10}(R_{cut}/V)$	24 (lim.)	18.19 ± 0.02	24 (lim.)	18.16 ± 0.01
I_H (%)	100 (fixed)	0.0	49.87	0.0
I_{He} (%)	-	27.17	10.92	28.60
I_N (%)	-	69.86	36.25	69.05
I_{Si} (%)	-	0.0	0.0	0.0
I_{Fe} (%)	-	2.97	2.96	2.35
D_J (N_J)	49.5 (24)		60.1 (24)	
$D_{X_{max}}$ $(N_{X_{max}})$	593.8 (329)		554.8 (329)	
D (N)	643.3 (353)		614.9 (353)	

Scenario B

Energy spectra at the sources

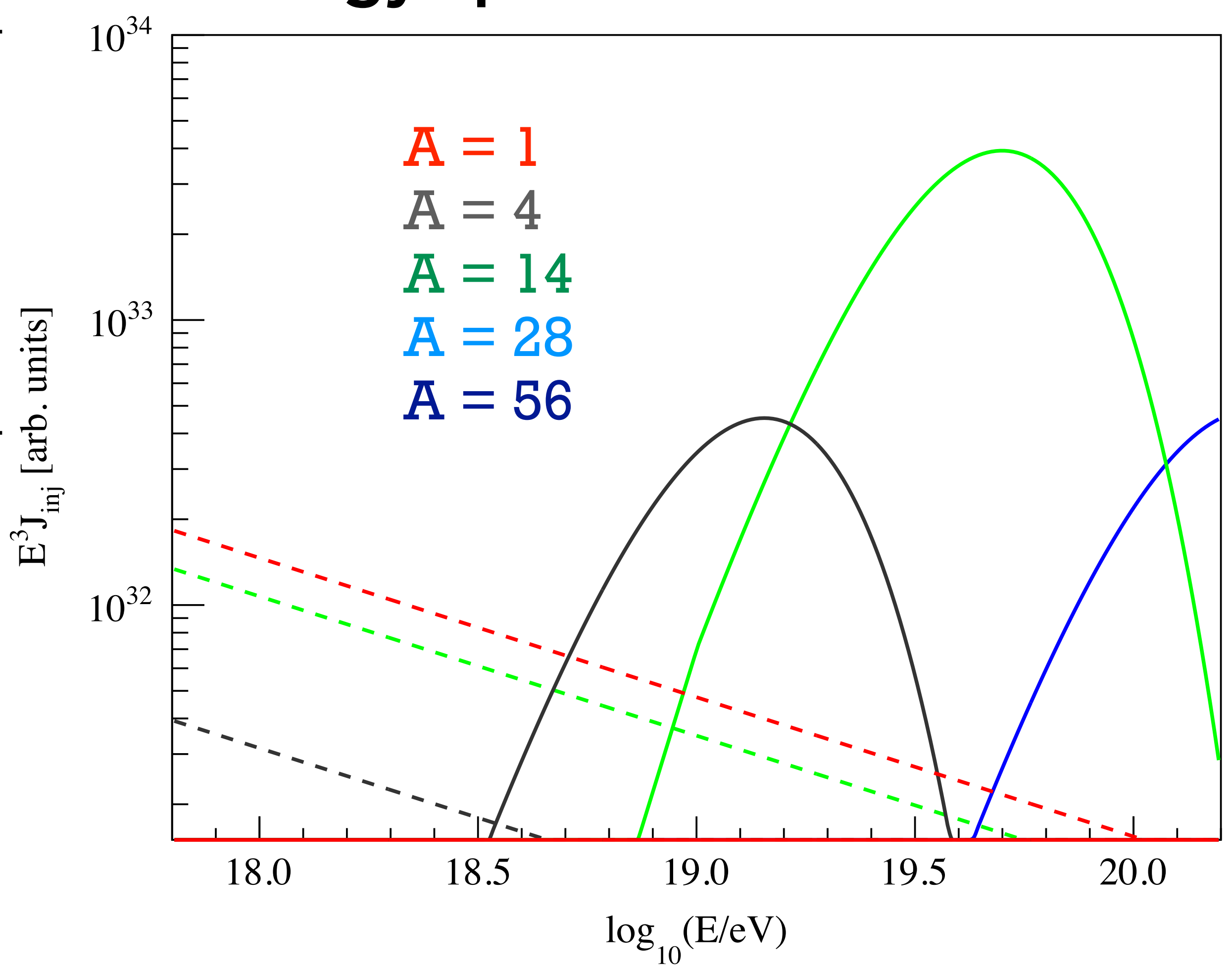

Energy spectrum at Earth

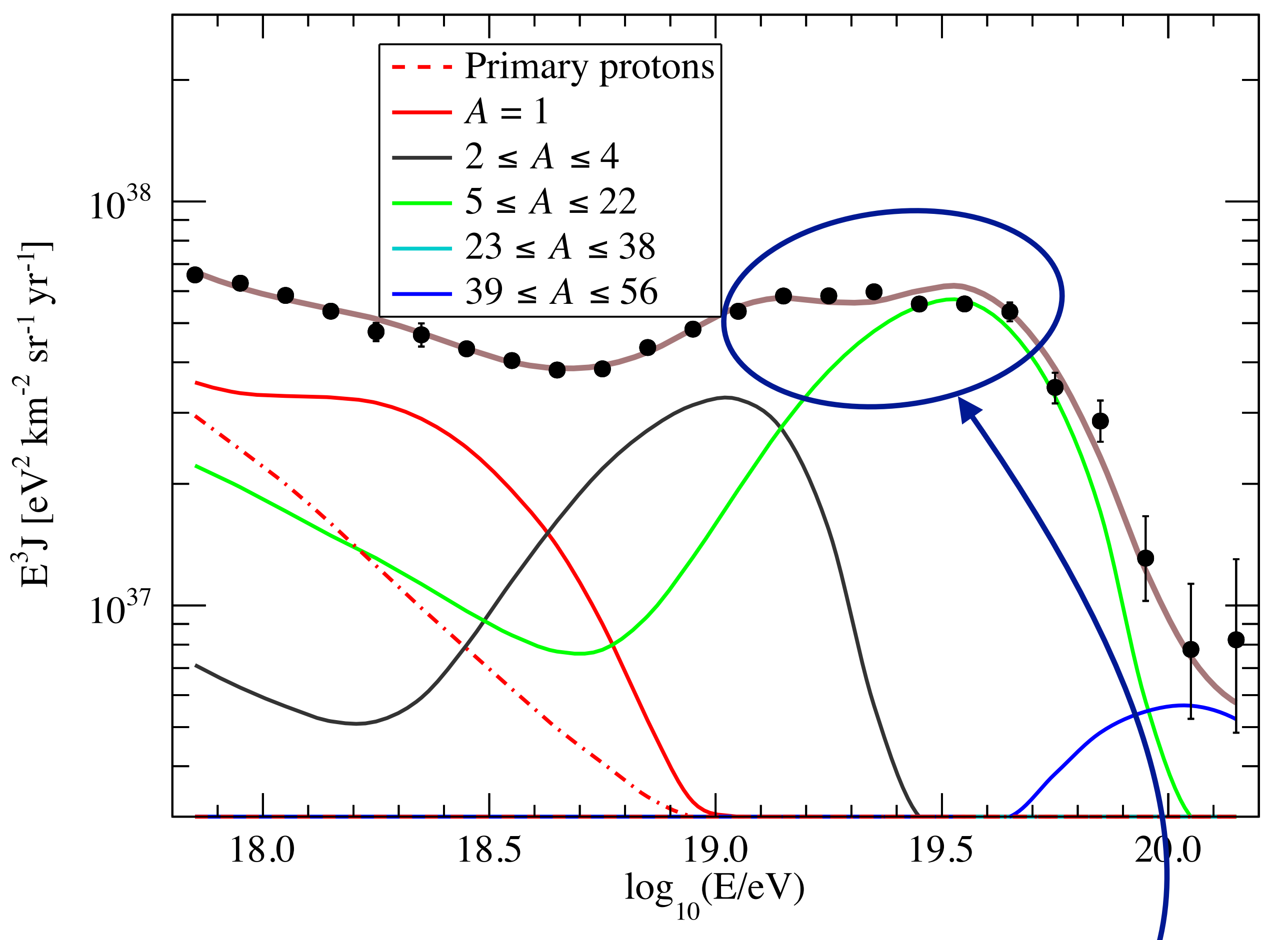

Very hard high-energy component dominated by N and He → to interpret the very pronounced spectrum features

- **Low-energy component:**
  - ✦ very soft energy spectrum → larger emissivity;
  - ✦ very high cutoff → not sensitive to the exact R_{cut} value (propagation effects are dominant)
- **High-energy component:**
  - ✦ hard energy spectrum, as in the above-ankle fit;
  - ✦ mixed mass composition (He and N are dominant)
  - ✦ relatively low cutoff → observed fluxes affected by it

Fit results in the two scenarios

Models configuration: Talys, Gilmore, EPOS-LHC

	Scenario A		**Scenario B**	
	Gal. contribution + EG component of pure p		Two EG mixed components	
Galactic contribution (at Earth)	N+Si		-	
J_0^{gal} [eV^{-1} km^{-2} sr^{-1} yr^{-1}]	$(1.07 \pm 0.06) \cdot 10^{-13}$		-	
$\log_{10}(R_{\mathrm{cut}}^{\mathrm{gal}}/\mathrm{V})$	17.48 ± 0.02		-	
f_{N} (%)	93.0		-	
EG components (at the sources)	Low energy	High energy	Low energy	High energy
$\mathcal{L}_0$ [erg Mpc^{-3} yr^{-1}]	$7.28 \cdot 10^{45}$	$4.4 \cdot 10^{44}$	$1.7 \cdot 10^{46}$	$4.5 \cdot 10^{44}$
γ	3.30 ± 0.05	-1.47 ± 0.12	3.49 ± 0.02	-1.98 ± 0.10
$\log_{10}(R_{\mathrm{cut}}/\mathrm{V})$	24 (lim.)	18.19 ± 0.02	24 (lim.)	18.16 ± 0.01
I_{H} (%)	100 (fixed)	0.0	49.87	0.0
I_{He} (%)	-	27.17	10.92	28.60
I_{N} (%)	-	69.86	36.25	69.05
I_{Si} (%)	-	0.0	0.0	0.0
I_{Fe} (%)	-	2.97	2.96	2.35
D_J (N_J)	49.5 (24)		60.1 (24)	
$D_{X_{\max}}$ ($N_{X_{\max}}$)	593.8 (329)		554.8 (329)	
D (N)	643.3 (353)		614.9 (353)	

Scenario B

Predicted fluxes at Earth

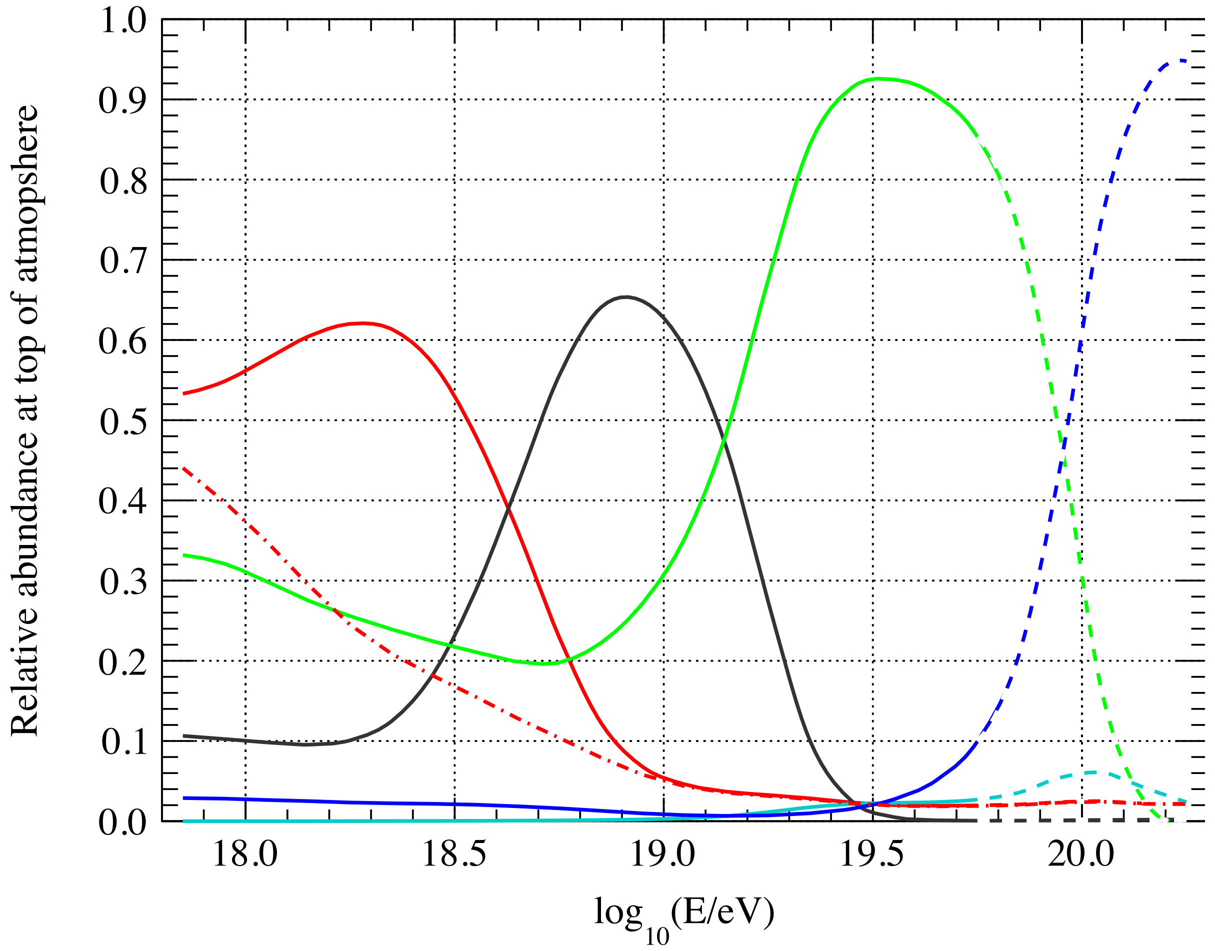

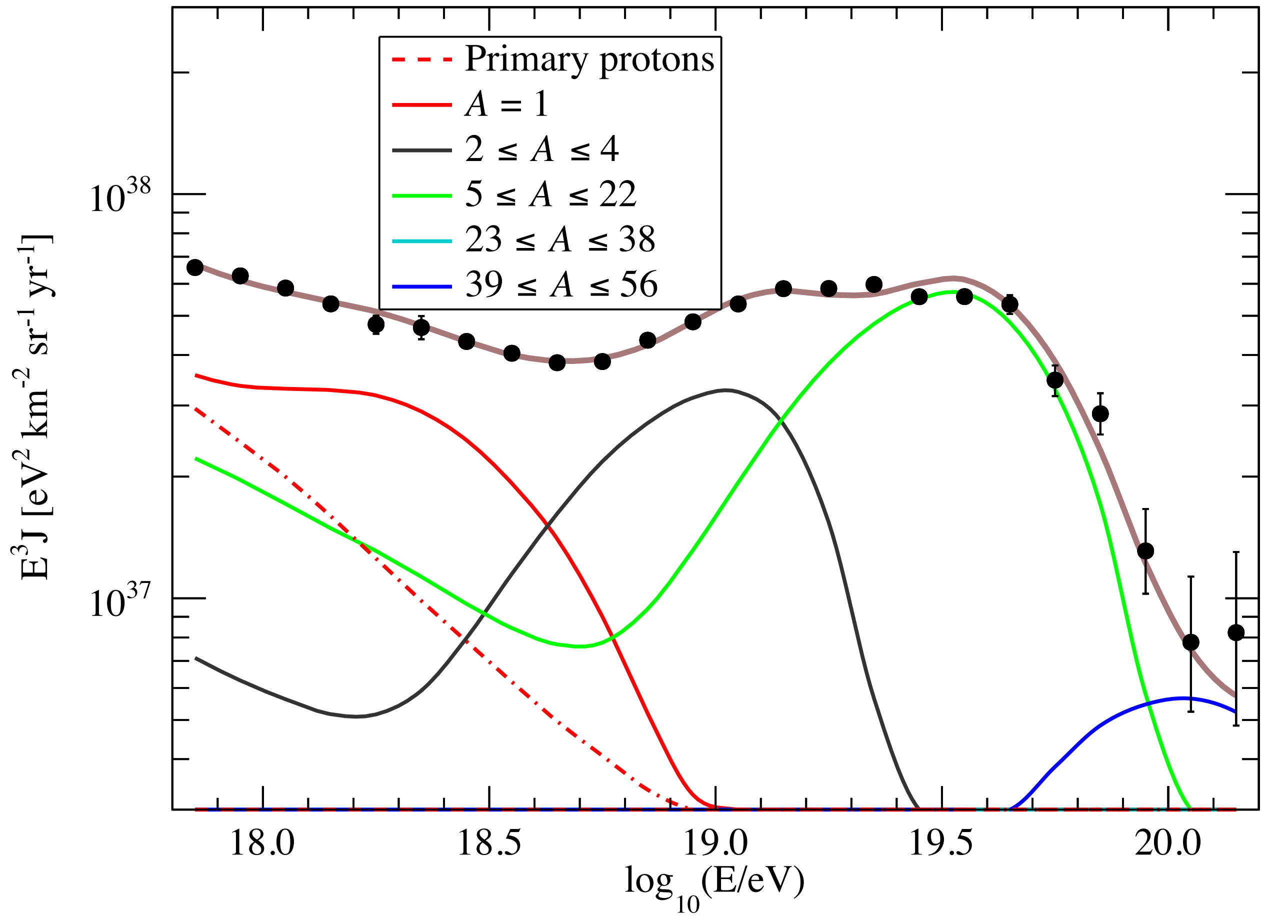

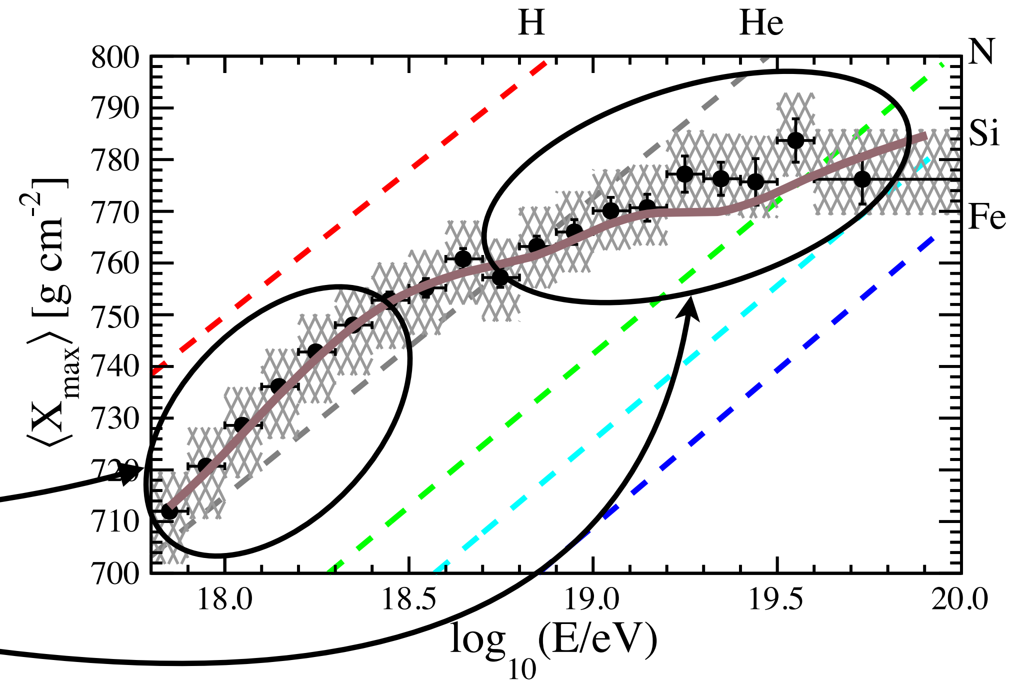

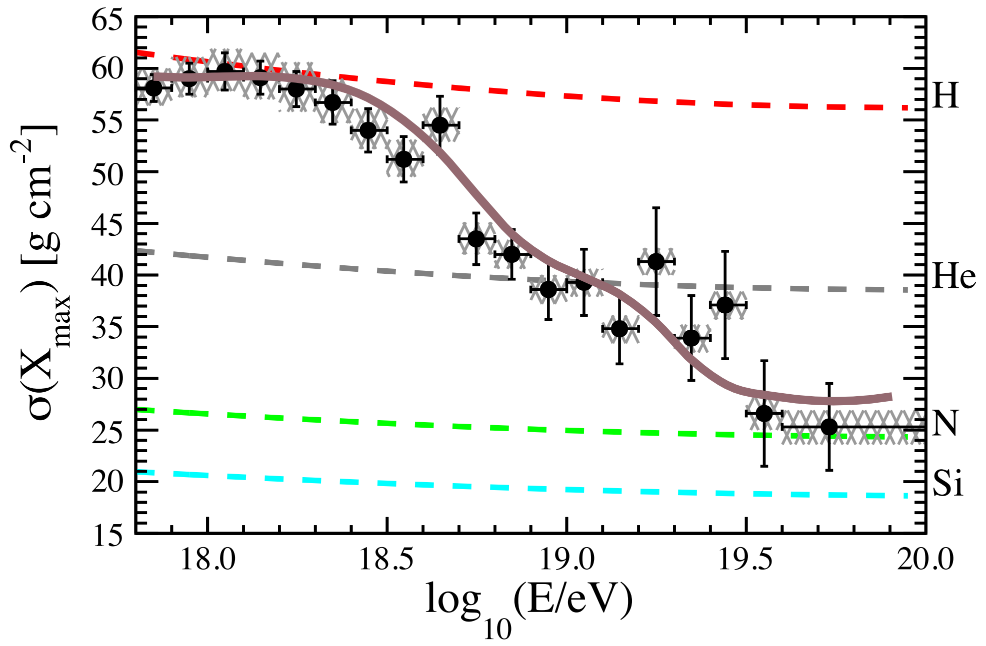

- ✦ **Low energy:** mixed composition dominated by H and N
- ✦ **High energy:** increasingly heavier mass composition, mass groups not much superposed

Fit results in the two scenarios

Models configuration: Talys, Gilmore, EPOS-LHC

	Scenario A Gal. contribution + EG component of pure p		**Scenario B** Two EG mixed components	
Galactic contribution (at Earth)	N+Si		-	
J_0^{gal} [eV^{-1} km^{-2} sr^{-1} yr^{-1}]	$(1.07 \pm 0.06) \cdot 10^{-13}$		-	
$\log_{10}(R_{cut}^{gal}/V)$	17.48 ± 0.02		-	
f_N (%)	93.0		-	
EG components (at the sources)	Low energy	High energy	Low energy	High energy
$\mathcal{L}_0$ [erg Mpc^{-3} yr^{-1}]	$7.28 \cdot 10^{45}$	$4.4 \cdot 10^{44}$	$1.7 \cdot 10^{46}$	$4.5 \cdot 10^{44}$
γ	3.30 ± 0.05	-1.47 ± 0.12	3.49 ± 0.02	-1.98 ± 0.10
$\log_{10}(R_{cut}/V)$	24 (lim.)	18.19 ± 0.02	24 (lim.)	18.16 ± 0.01
I_H (%)	100 (fixed)	0.0	49.87	0.0
I_{He} (%)	-	27.17	10.92	28.60
I_N (%)	-	69.86	36.25	69.05
I_{Si} (%)	-	0.0	0.0	0.0
I_{Fe} (%)	-	2.97	2.96	2.35
D_J (N_J)	49.5 (24)		60.1 (24)	
$D_{X_{max}}$ ($N_{X_{max}}$)	593.8 (329)		554.8 (329)	
D (N)	643.3 (353)		614.9 (353)	

Scenario B

Predicted fluxes at Earth

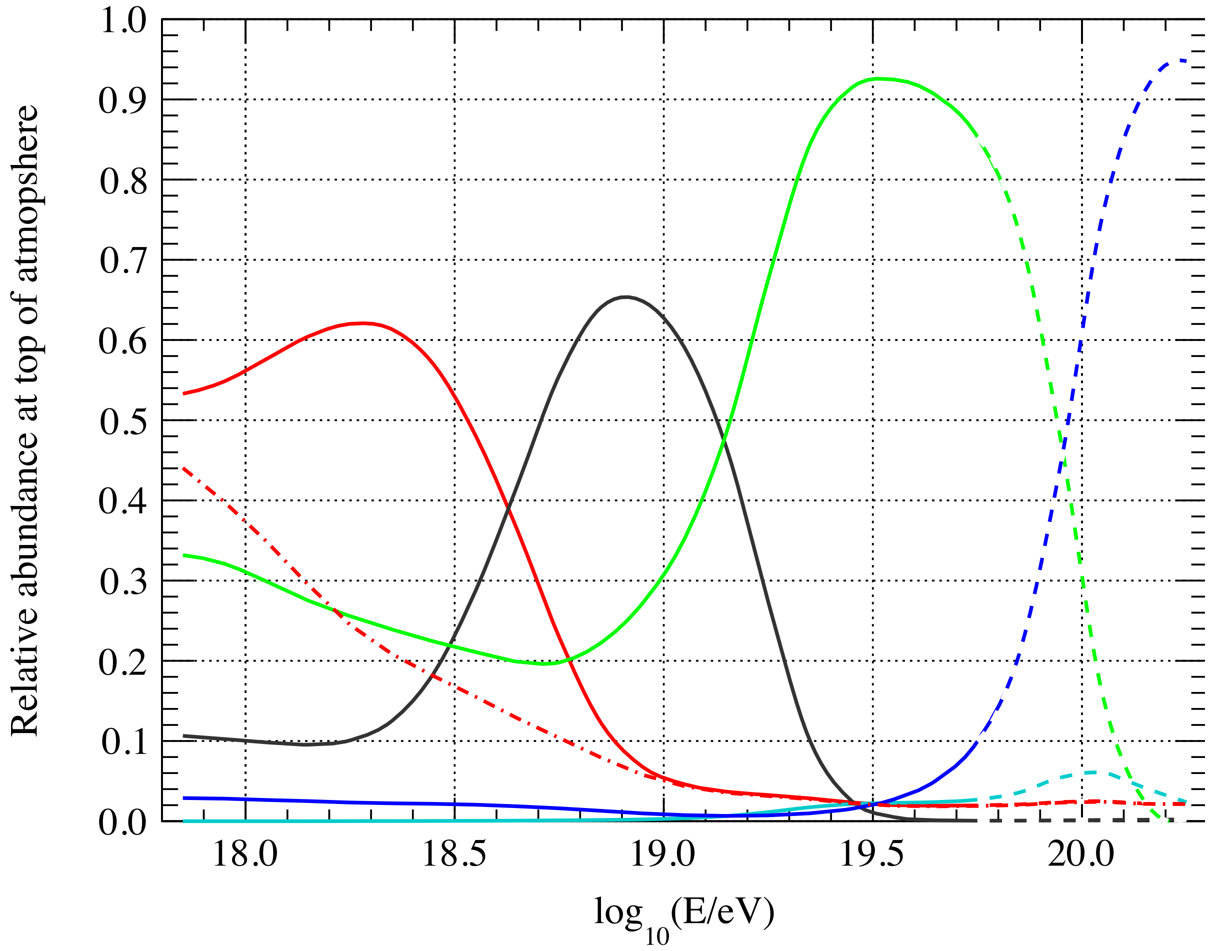

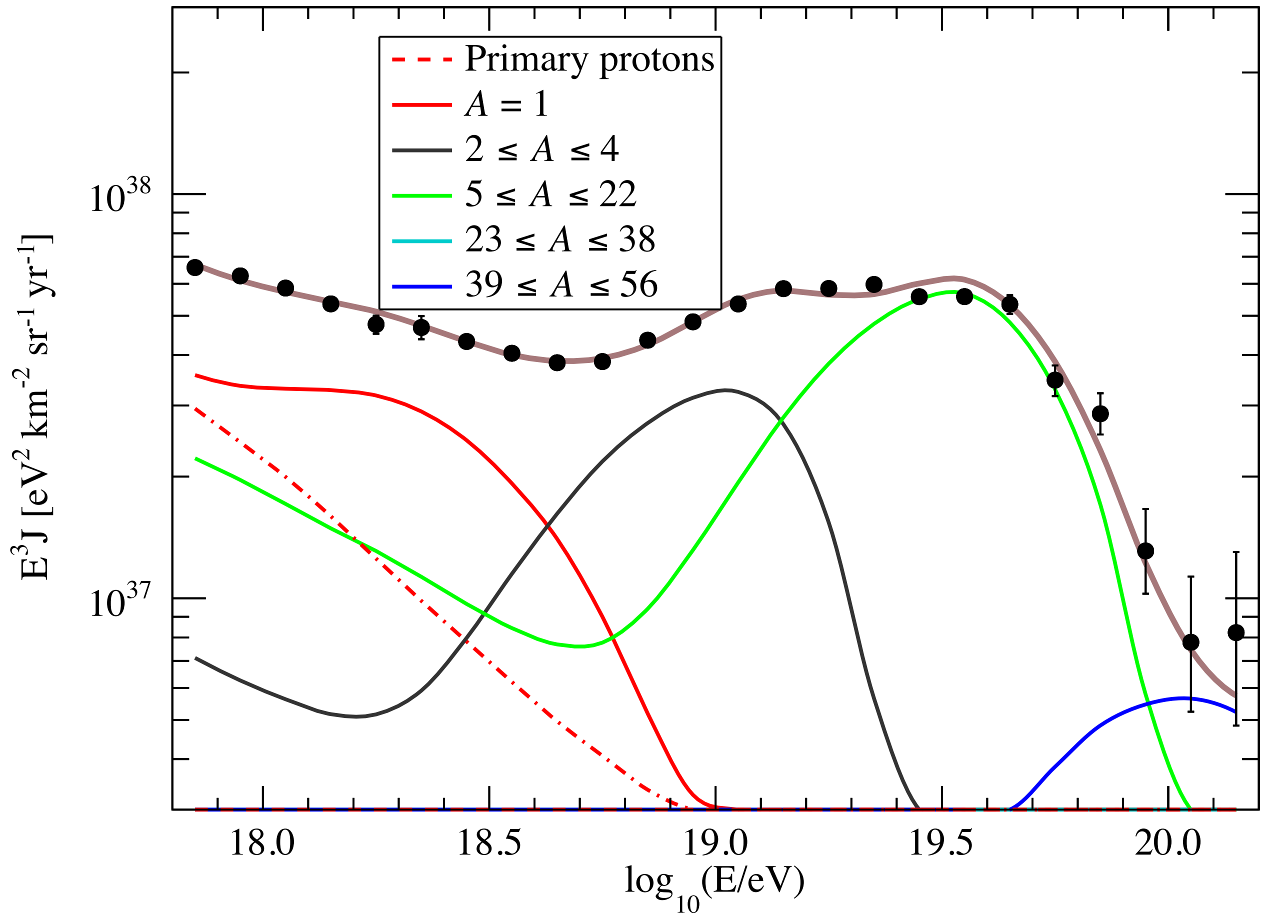

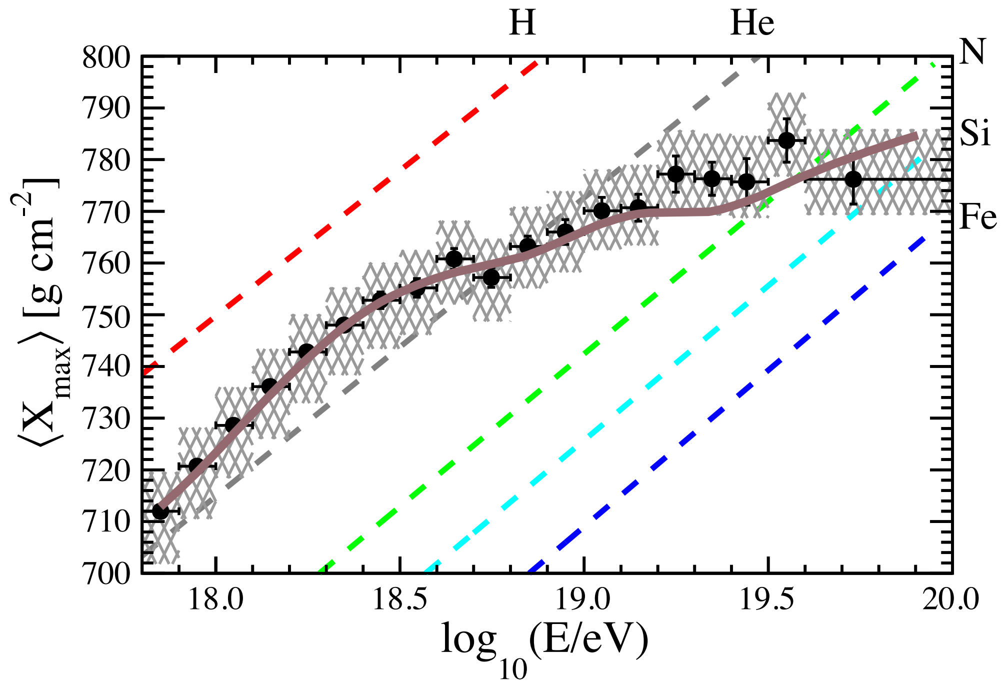

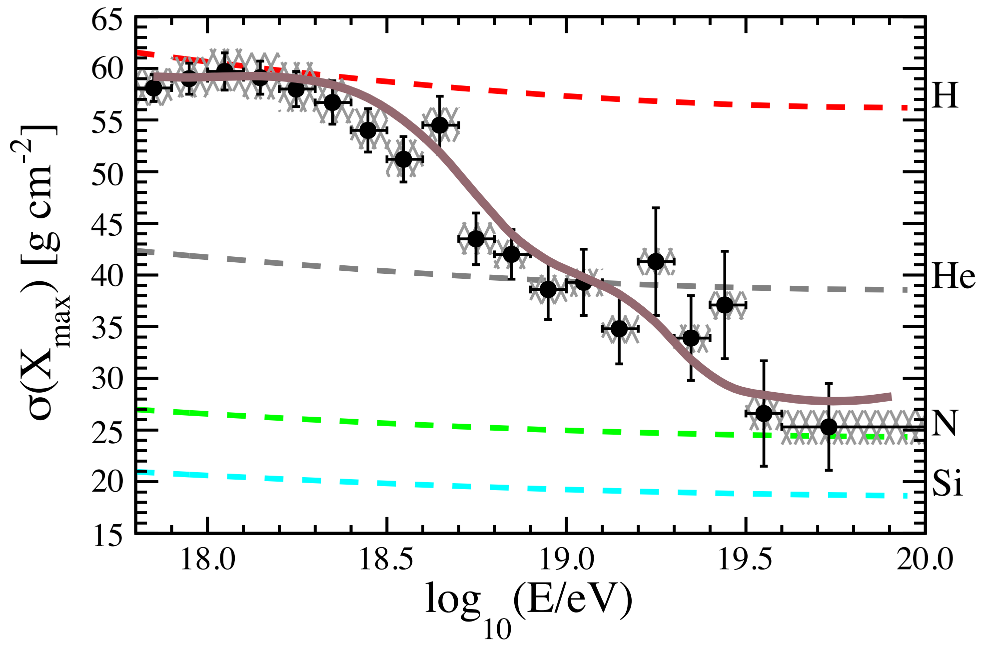

Differences between the two scenarios within the systematic uncertainties

→ further investigations of the Galactic contribution to possibly define a favoured scenario

Effect of the systematic uncertainties

Experimental systematic uncertainties:

- **Energy scale:** $\sigma_{sys}(E)/E = 14\,\%$
- **X_{max} scale:** $\sigma_{sys}(X_{max}) = 6 \div 9 \text{ g cm}^{-2}$

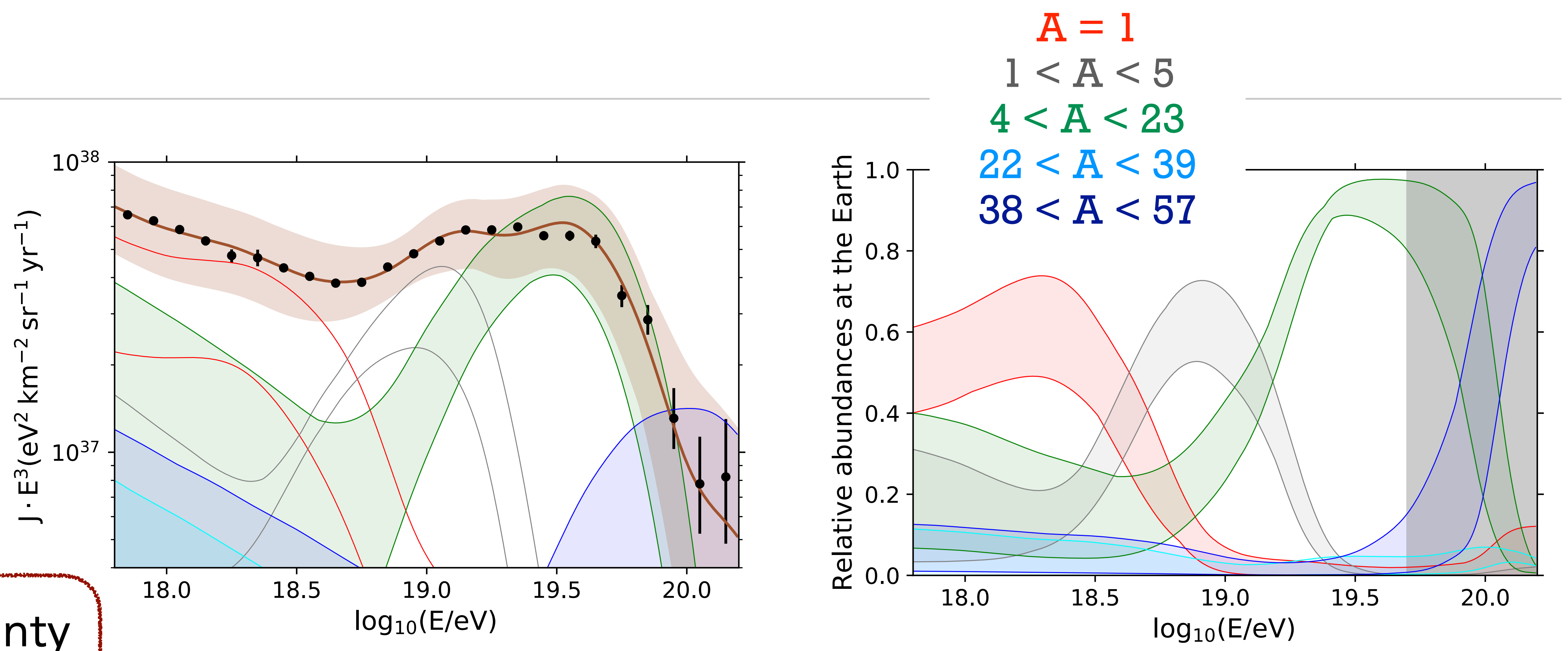

- *Large band around the total flux* due to the energy scale uncertainty → impact mainly on the estimated J_0 (and emissivity of sources)
- The ***strongest impact*** on the predictions is the one from the X_{max} scale

Systematic uncertainties from models:

Hadronic interaction model: Sibyll2.3d/EPOS-LHC/intermediate models (with a nuisance parameter)

Propagation models: Talys/PSB; Gilmore/Dominguez

(fit repeated considering different model configurations)

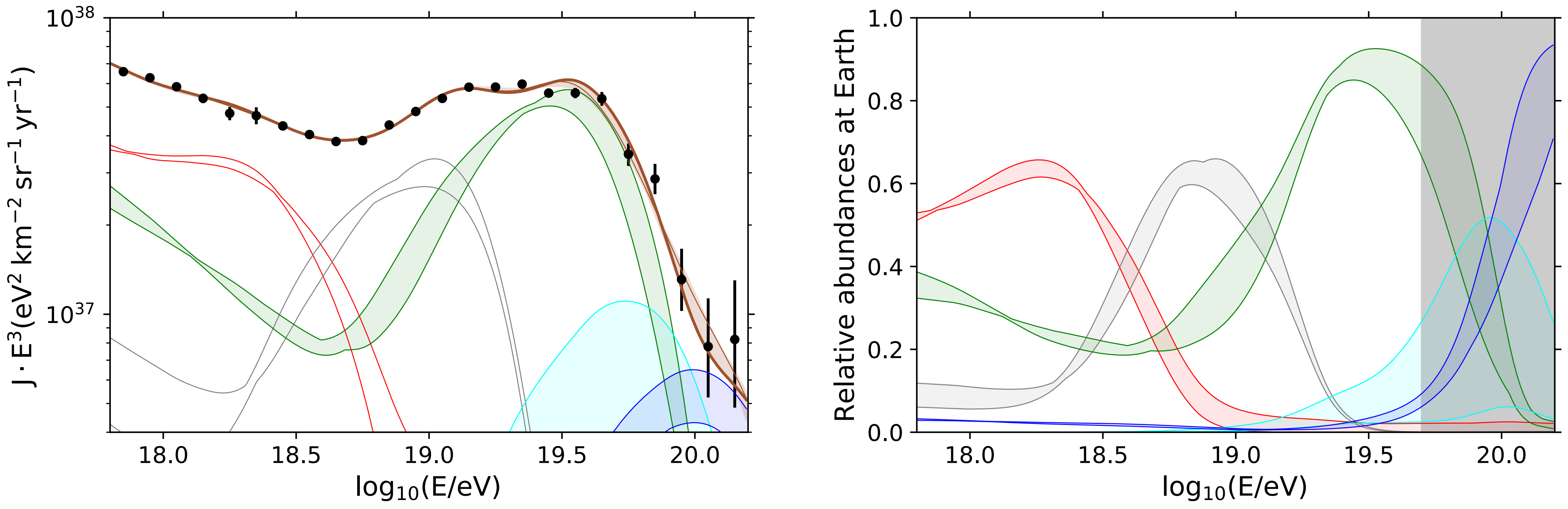

- *EPOS-LHC or models compatible with it are always preferred*

  → **HIM choice: stronger impact on D and on the predictions at Earth**

Effect of the systematic uncertainties

Experimental systematic uncertainties:

- **Energy scale:** $\sigma_{sys}(E)/E = 14\,\%$
- **X_{max} scale:** $\sigma_{sys}(X_{max}) = 6 \div 9\ \mathrm{g\ cm^{-2}}$

A = 1
1 < A < 5
4 < A < 23
22 < A < 39
38 < A < 57

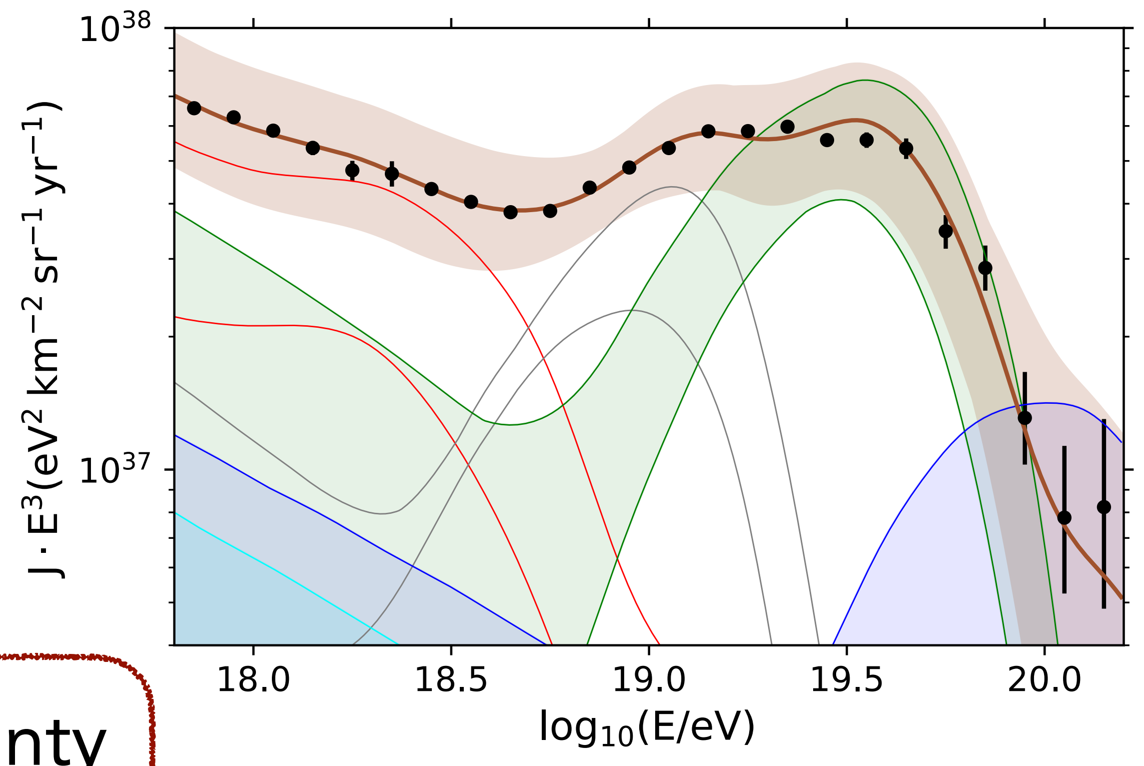

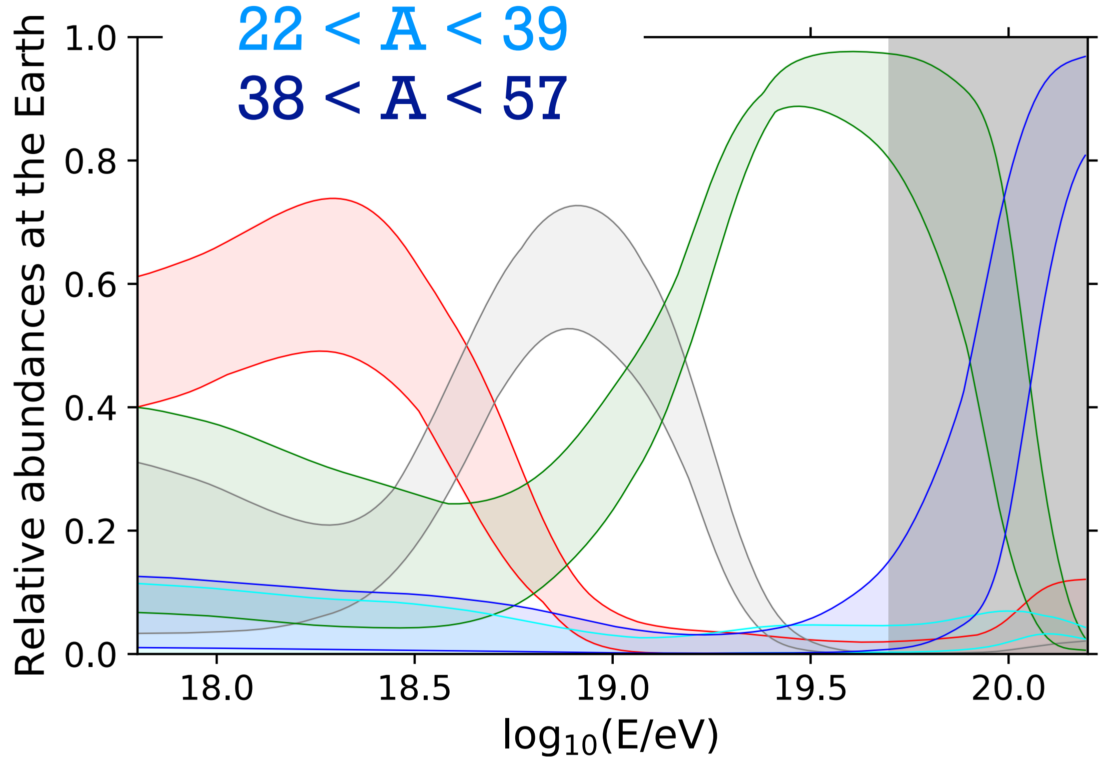

- *Large band around the total flux* due to the energy scale uncertainty → impact mainly on the estimated J_0 (and emissivity of sources)
- The ***strongest impact*** on the predictions is the one from the X_{max} scale

Systematic uncertainties from models:

<u>**Hadronic interaction model:**</u> Sibyll2.3d/EPOS-LHC/intermediate models (with a nuisance parameter)

<u>**Propagation models:**</u> Talys/PSB; Gilmore/Dominguez

(fit repeated considering different model configurations)

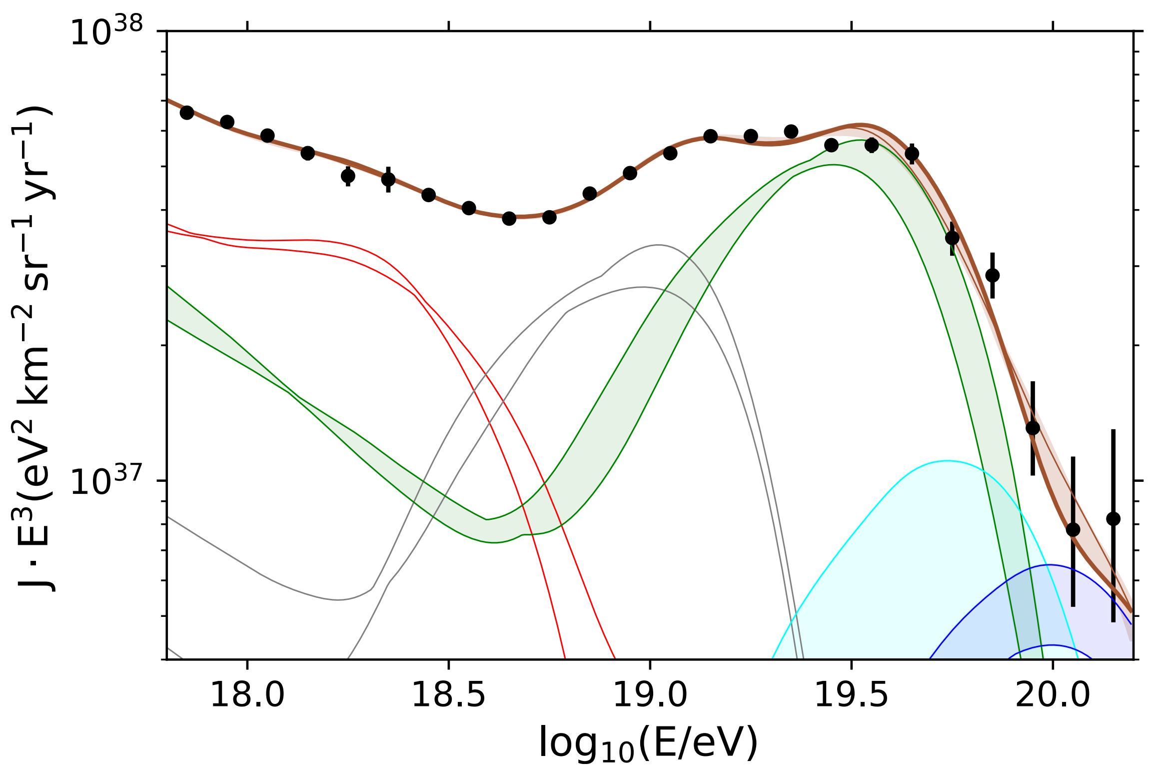

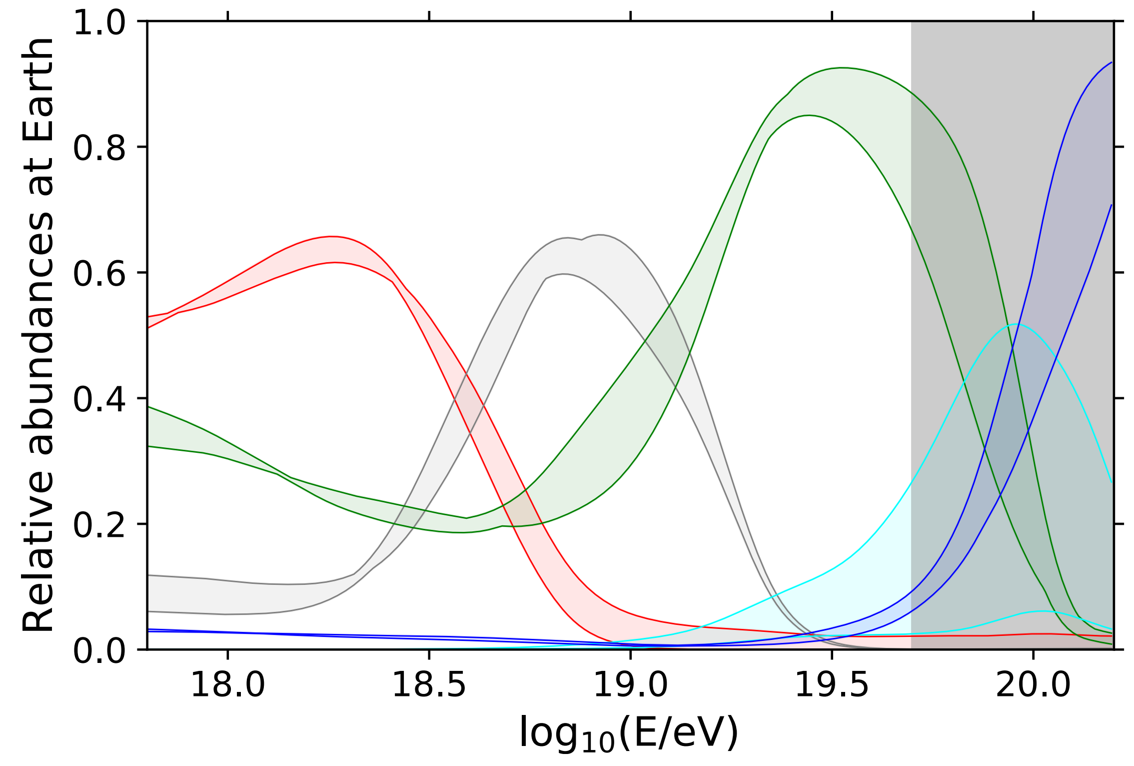

- <u>*EPOS-LHC or models compatible with it are always preferred*</u>

  → **HIM choice: stronger impact on D and on the predictions at Earth**

<u>**The dominant effect on the the predicted fluxes and on the deviance is the one from the experimental uncertainties**</u>

Effect of the source evolution

- Three possible source evolution: m=-3 (TDE-like), m=3.5 (SF-like), m=5 (AGN-like)
- All the combinations are considered for the two EG populations

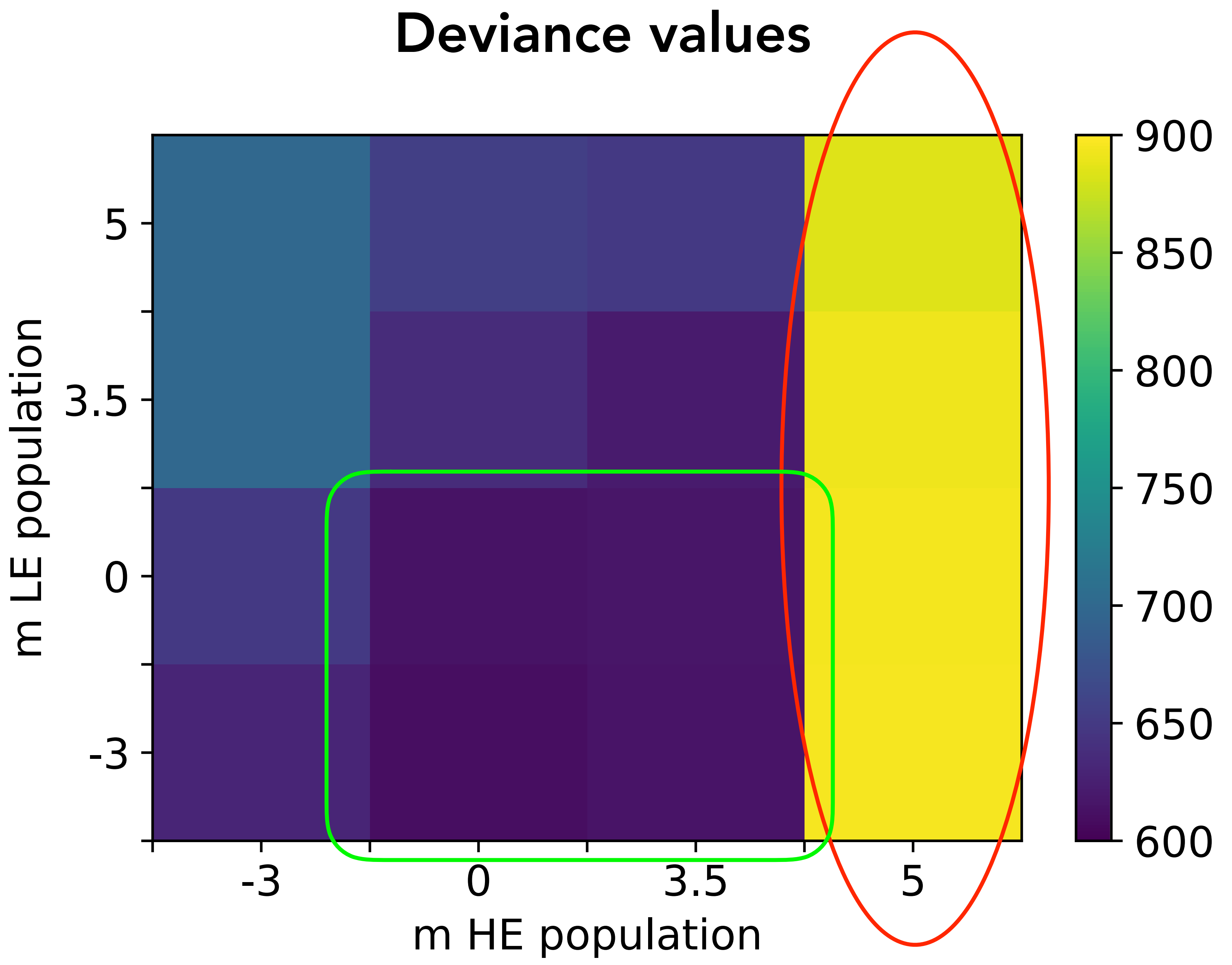

An AGN-like source evolution (m~5 at small z) for the HE population is disfavoured

The other scenarios exhibit differences encompassed within the systematic uncertainties effect

→ **no scenario is favoured over the others**

Some of them have deviances comparable the one without source evolution (D~615):

- m=0/m=3.5 source evolution for the HE component
- m=-3/m=0 source evolution for the LE component

Conclusions

The energy spectrum and mass composition data for E>$10^{17.8}$ eV can be interpreted by the superposition of different components

- **Region above the ankle:**
  - ✳ *Very hard energy spectrum at the sources* → describe the very **pronounced spectral features** and the rather **narrow X_{max} distributions**
  - ✳ ***Hardening wrt JCAP2017*** ($\gamma < 0$) but it is comparable to the effects of the systematic uncertainties
    - deviance profile approximately flat for $R_{\rm cut} \leq 5 \cdot 10^{18}$ eV and $\gamma \leq 1$
  - ✳ **Rigidity cutoff < $10^{18.5}$ eV** → the cutoff at the sources affect the observed fluxes, but ***propagation energy losses*** NOT negligible

- **Alternative scenarios providing similar results for the region below the ankle:**
  - ✳ One additional protons EG component + an intermediate-mass Galactic contribution at the Earth
    - A heavy composition is disfavoured (D~1000 if it is Si-dominated), a **N-dominated composition is preferred**
  - ✳ One additional mixed component ejected by another population of EG sources
  - ✳ **In both cases the additional EG component has:**
    - Very soft energy spectrum → larger emissivity
    - Very high rigidity cutoff (not constrained by the fit)

Conclusions

- All the results are prone to the effect of the ***systematic uncertainties***

  ✳ **Experimental**: X_{max} scale, (acceptance, resolution) and energy scale

  ✳ **From models**: propagation and hadronic interaction models uncertainties

  → **strongest impact from the X_{max} uncertainties on the predictions at Earth**

  → **minor impact of the model uncertainties, dominated by the hadronic interaction model choice (*EPOS-LHC always preferred*)**

- **Source evolution effect**: some scenarios can be excluded but no favoured one can be selected

  → a strong evolution (e.g. m~5) for the HE component is disfavoured by our data (too many predicted low-energy particles to be compensated by a hardening of the HE energy spectrum)

The low-energy enhancements of the Observatory will allow in the future to go to even lower energies → explore the transition region

Thank you for your attention

Backup slides

Back-up slides content:

- Overdensity correction effect
- Experimental systematic uncertainties
  - ✳ From the X_{max} scale
  - ✳ From the energy scale
- Systematic uncertainties from models
- Fractions of the energy density integral
- Systematic uncertainties effect in JCAP2017
- Mean rigidity vs energy

Taking into account the overdensity of nearby sources

In the simplest case:

- No source evolution
- Sources uniformly distributed in the comoving volume up to z_{max}

The Milky Way belongs to a cluster of Galaxy → $\rho_{loc} > \rho_{avg}$

→ **overdensity correction** to the weight of each event produced at r < 28.5 Mpc (z < 0.007)

$$\frac{\rho_{loc}}{\rho_{avg}} = 1 + \left(\frac{r_0}{r(z)}\right)^{\lambda} \qquad \lambda = 1.66, \quad r_0 = 5.4\ \mathrm{Mpc}$$

[J.J.Condon et al., (2019)]

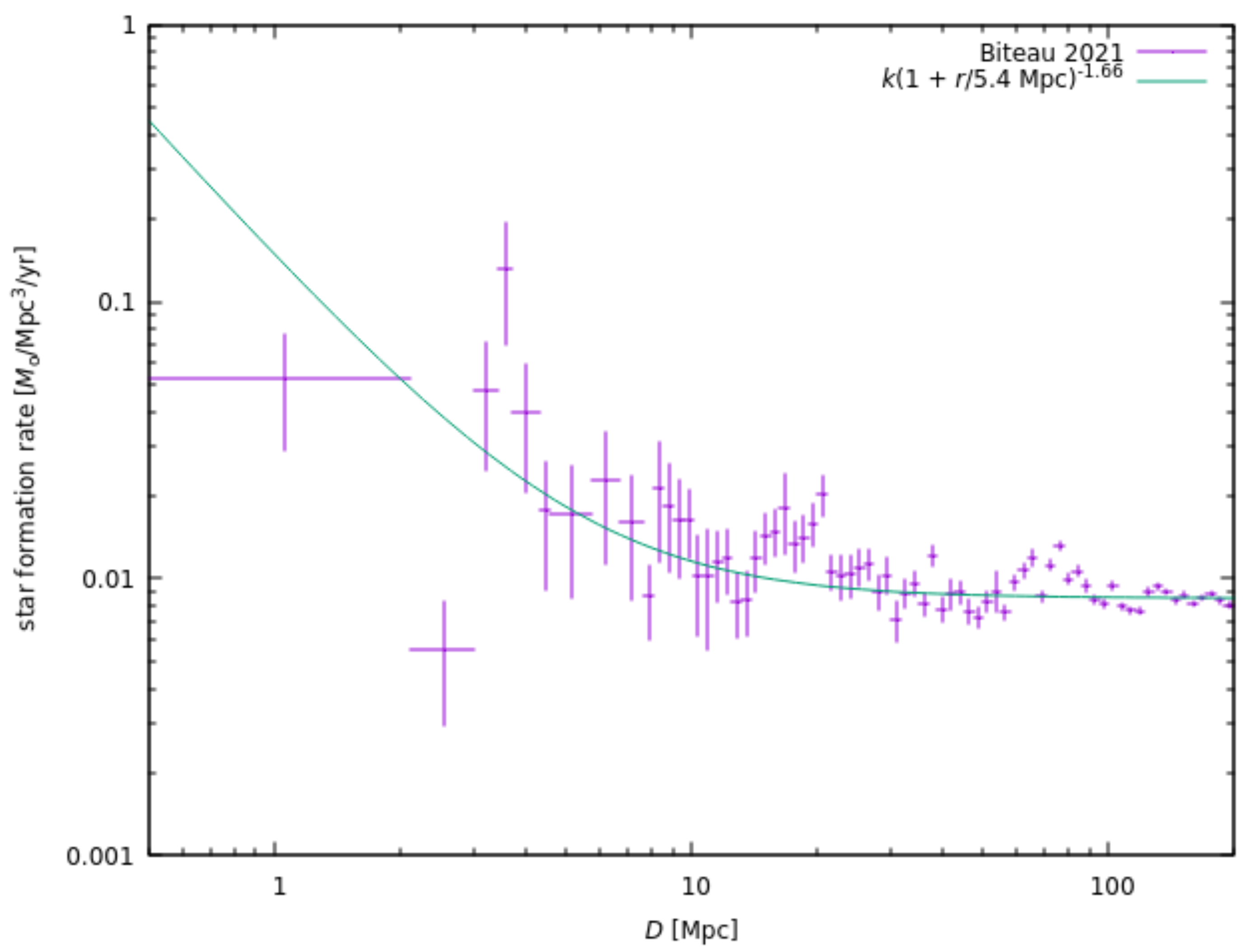

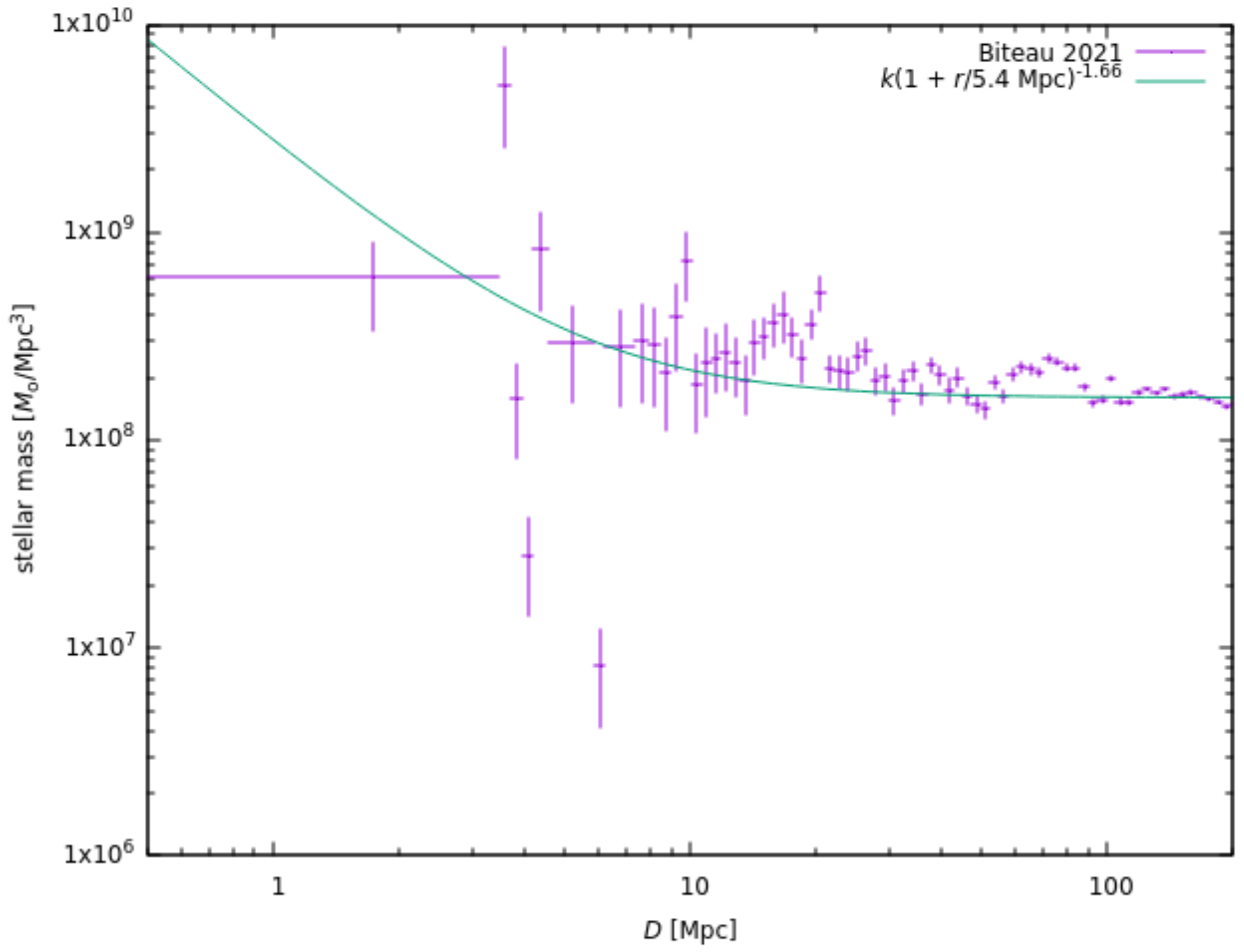

Good agreement with distributions of stellar mass and SFR densities (see Biteau 2021)

Effect of the overdensity correction on the combined fit results

Models configuration: Talys, Gilmore, EPOS-LHC

Without the overdensity correction

	LE	**HE**
γ	3.52 ± 0.03	-2.21 ± 0.11
$\log (R_{cut}/V)$	24.0 (fixed)	18.13 ± 0.01
I_H (%)	50.09	0.0
I_{He} (%)	8.74	24.31
I_N (%)	38.17	63.01
I_{Si} (%)	0.0	9.67
I_{Fe} (%)	3.01	3.01
D_{Xmax} (N)	**562.0 (329)**	
D_J (N)	**51.6 (24)**	
D_{tot} (N)	**613.6 (353)**	

With the overdensity correction

	LE	**HE**
γ	3.49 ± 0.03	-1.98 ± 0.10
$\log (R_{cut}/V)$	24.0 (fixed)	18.16 ± 0.01
I_H (%)	49.84	0.0
I_{He} (%)	10.73	28.09
I_N (%)	36.54	69.61
I_{Si} (%)	0.0	0.0
I_{Fe} (%)	2.88	2.29
D_{Xmax} (N)	**554.8 (329)**	
D_J (N)	**60.1 (24)**	
D_{tot} (N)	**614.9 (353)**	

Effect of the systematic uncertainties

Experimental systematic uncertainties:

- **Energy scale:** $\sigma_{sys}(E)/E = 14\,\%$
- **X_{max} scale:** $\sigma_{sys}(X_{max}) = 6 \div 9\ \mathrm{g\ cm^{-2}}$

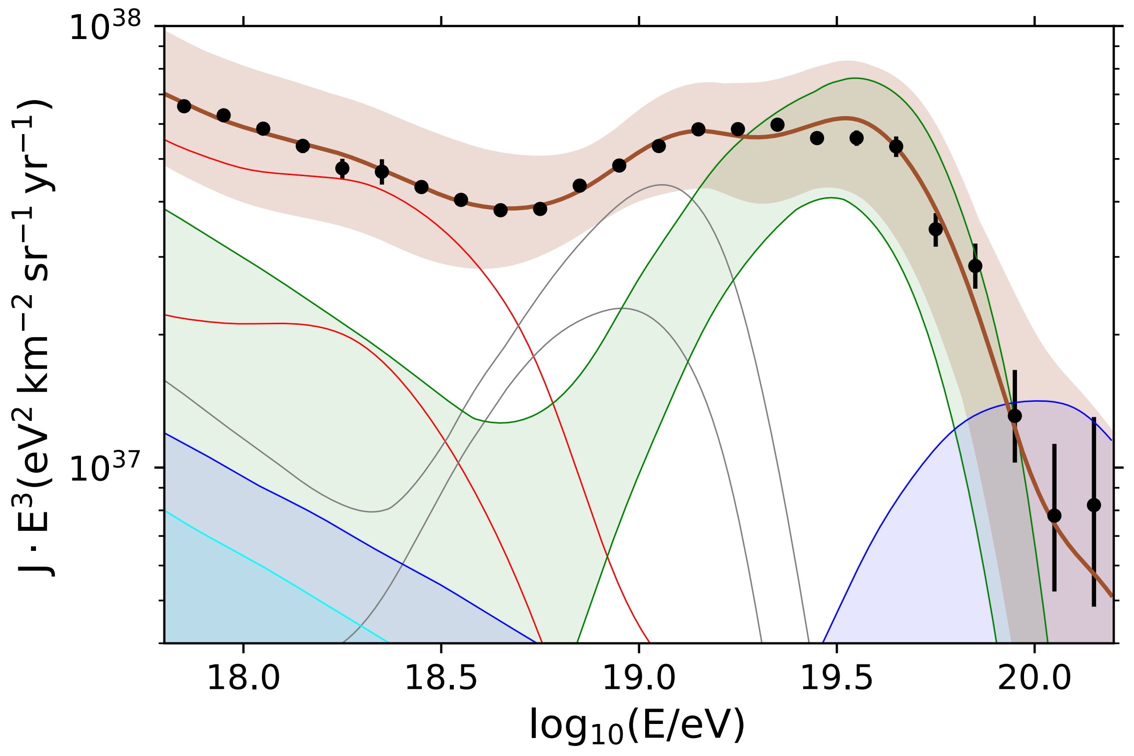

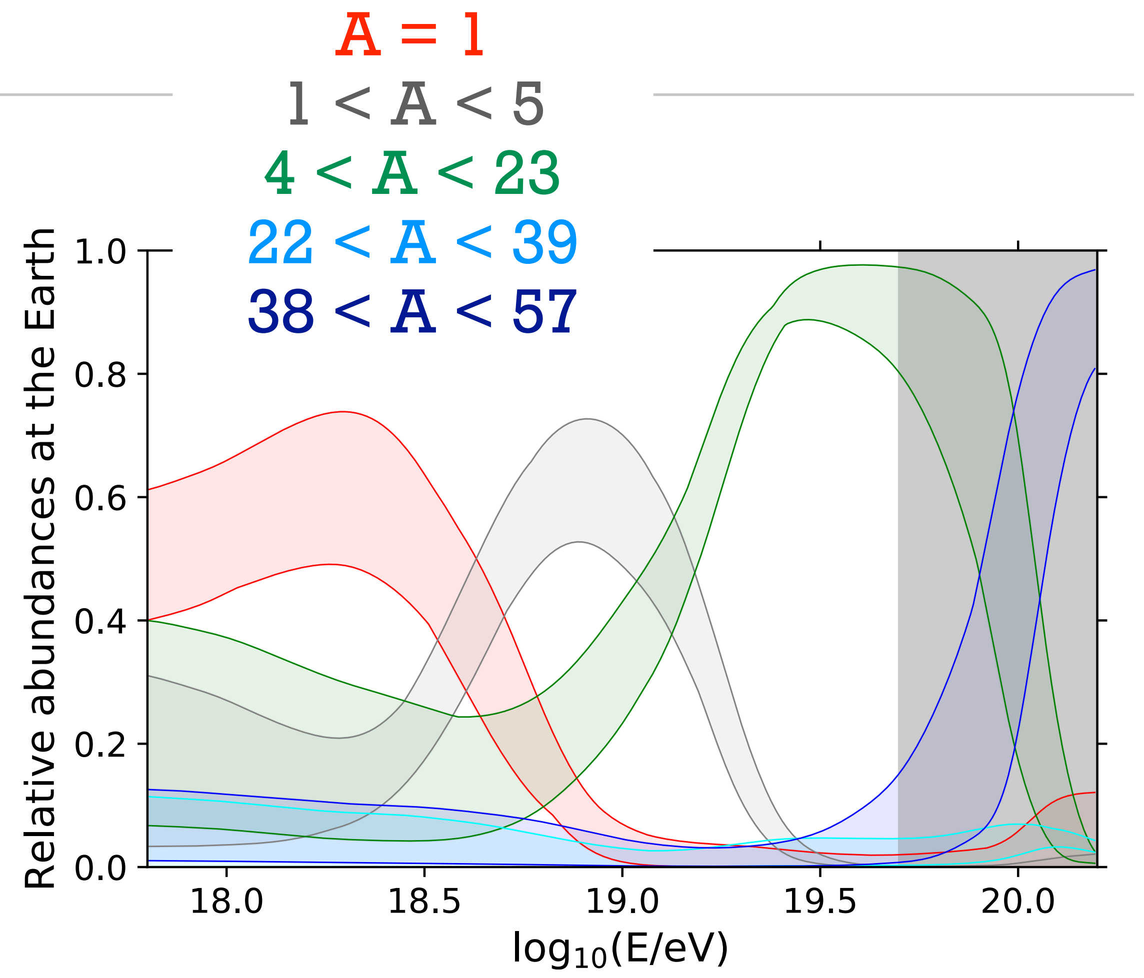

ΔX_{max}	$\Delta E/E$	D_J	$D_{X_{max}}$	D_{tot}
	-14%	52.5	578.3	630.9
$-1\sigma_{syst}$	0	71.7	595.2	666.9
	+14%	64.9	609.3	674.2
	-14%	53.5	581.3	634.8
0	0	60.1	554.8	614.9
	+14%	70.6	548.8	619.5
	-14%	79.1	714.2	793.3
$+1\sigma_{syst}$	0	80.8	555.4	736.2
	+14%	82.4	615.7	698.2

- ***Large band around the total flux*** due to the energy scale uncertainty → impact mainly on the estimated J_0 (and emissivity of sources)
- The ***strongest impact*** on the predicted fluxes and on the deviance is due to the X_{max} scale uncertainty

Effect of the experimental uncertainties: X_{max} scale

Models configuration: Talys, Gilmore, EPOS-LHC

$\Delta X_{\max}/\sigma_{\text{syst}}$	-1		0		$+1$	
Component	LE	HE	LE	HE	LE	HE
γ	3.47 ± 0.02	-1.83 ± 0.15	3.49 ± 0.02	-1.98 ± 0.10	3.54 ± 0.04	-2.24 ± 0.14
$\log_{10}(R_{\text{cut}}/\text{V})$	19.4 ± 0.2	18.15 ± 0.02	24 (lim.)	18.16 ± 0.01	24 (lim.)	18.15 ± 0.01
I_{H} (%)	36.48	$O(10^{-8})$	49.87	$O(10^{-7})$	56.07	3.46
I_{He} (%)	13.20	21.76	10.92	28.60	23.30	29.93
I_{N} (%)	30.73	74.64	36.25	69.05	19.57	65.45
I_{Si} (%)	11.86	$O(10^{-7})$	$O(10^{-6})$	$O(10^{-7})$	$O(10^{-7})$	$O(10^{-6})$
I_{Fe} (%)	7.74	3.60	2.96	2.35	1.07	1.16
D_J (N_J)	71.7 (24)		60.1 (24)		80.8 (24)	
$D_{X_{\max}}$ $(N_{X_{\max}})$	595.2 (329)		554.8 (329)		555.4 (329)	
D_{tot} (N)	666.9 (353)		614.9 (353)		736.2 (353)	

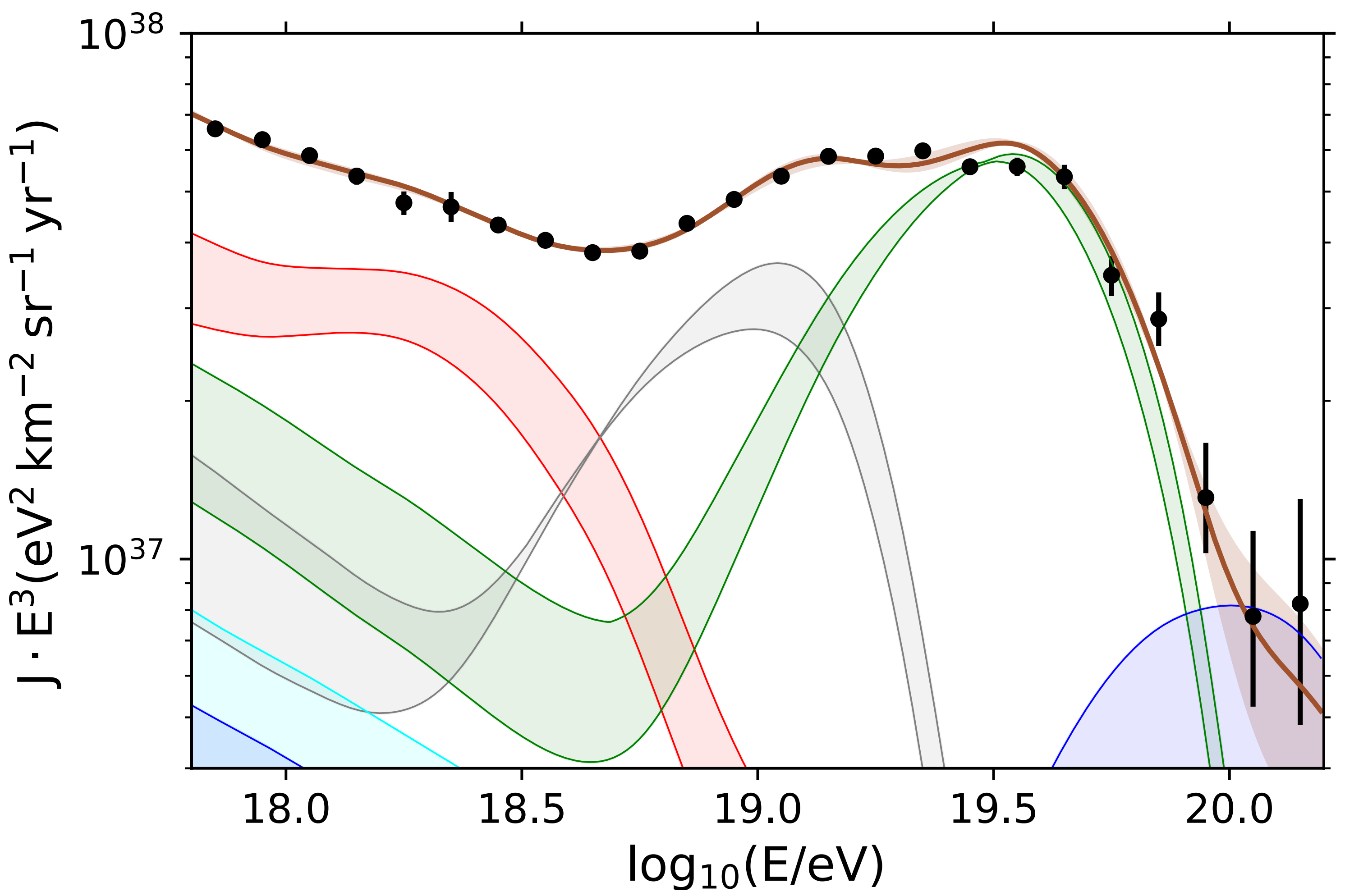

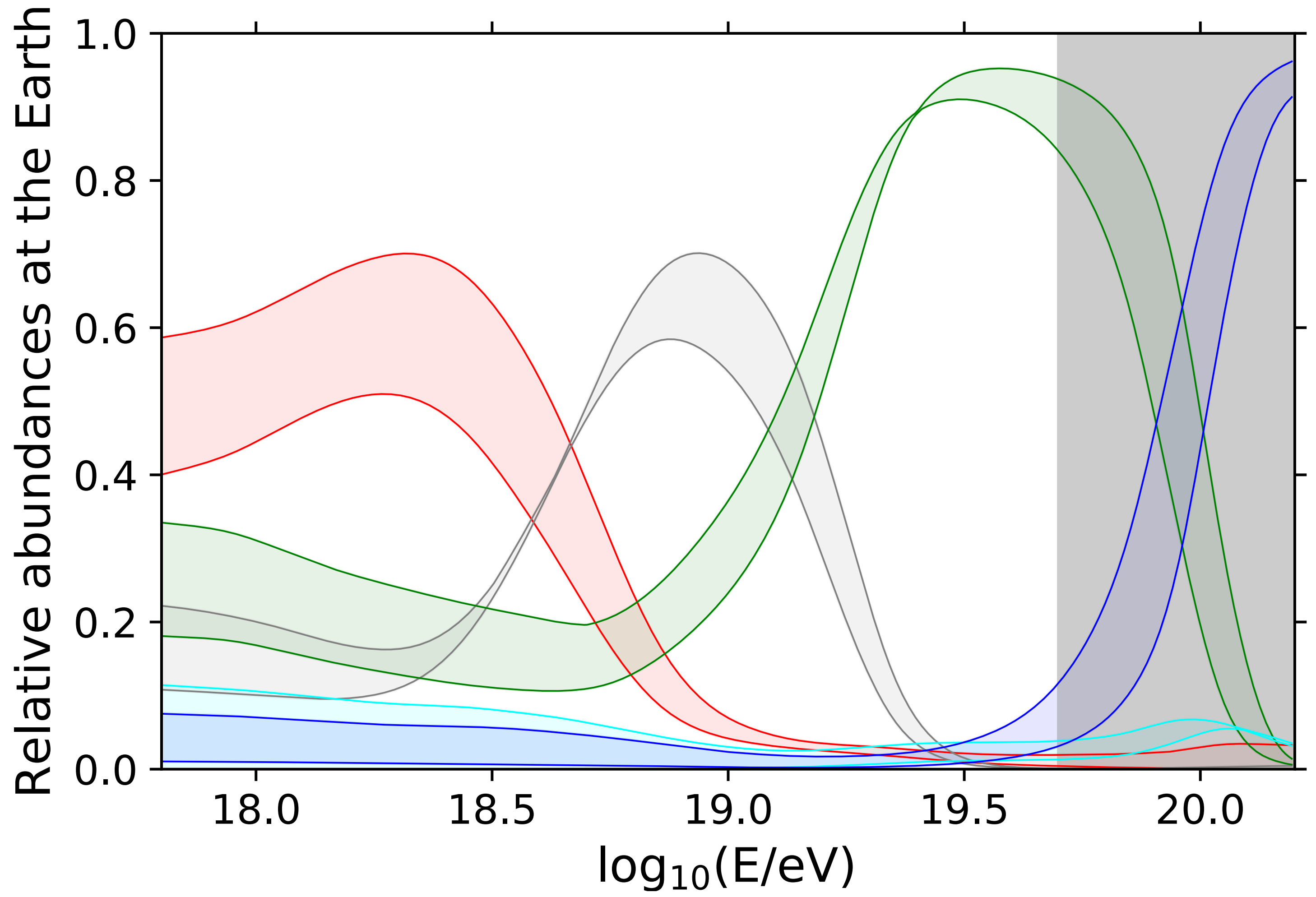

Effect of the experimental uncertainties: energy scale

Models configuration: Talys, Gilmore, EPOS-LHC

$\Delta E/\sigma_{\rm syst}$	−1		0		+1	
Component	LE	HE	LE	HE	LE	HE
γ	3.51 ± 0.03	-1.91 ± 0.13	3.49 ± 0.02	-1.98 ± 0.10	3.48 ± 0.02	-1.87 ± 0.12
$\log_{10}(R_{\rm cut}/{\rm V})$	24 (lim.)	18.13 ± 0.02	24 (lim.)	18.16 ± 0.01	24 (lim.)	18.19 ± 0.01
$I_{\rm H}$ (%)	51.45	1.09	49.87	$O(10^{-7})$	48.15	$O(10^{-7})$
$I_{\rm He}$ (%)	20.67	34.69	10.92	28.60	4.35	21.93
$I_{\rm N}$ (%)	26.20	62.97	36.25	69.05	42.52	74.43
$I_{\rm Si}$ (%)	$O(10^{-6})$	$O(10^{-6})$	$O(10^{-6})$	$O(10^{-7})$	$O(10^{-7})$	$O(10^{-9})$
$I_{\rm Fe}$ (%)	1.68	1.24	2.96	2.35	4.98	3.64
D_J (N_J)	53.5 (24)		60.1 (24)		70.6 (24)	
$D_{X_{\rm max}}$ ($N_{X_{\rm max}}$)	581.3 (329)		554.8 (329)		548.8 (329)	
$D_{\rm tot}$ (N)	634.8 (353)		614.9 (353)		619.5 (353)	

$\Delta E/\sigma_{\rm syst} = 0$: $\mathscr{L}_0(E > 10^{17}\ {\rm eV}) = 1.7 \cdot 10^{46}\ {\rm erg\ Mpc^{-3}\ yr^{-1}}$ $\mathscr{L}_0(E > 10^{17}\ {\rm eV}) = 4.5 \cdot 10^{44}\ {\rm erg\ Mpc^{-3}\ yr^{-1}}$

$\Delta E/\sigma_{\rm syst} = -1$: $\mathscr{L}_0(E > 10^{17}\ {\rm eV}) = 1.2 \cdot 10^{46}\ {\rm erg\ Mpc^{-3}\ yr^{-1}}$ $\mathscr{L}_0(E > 10^{17}\ {\rm eV}) = 3.5 \cdot 10^{44}\ {\rm erg\ Mpc^{-3}\ yr^{-1}}$

$\Delta E/\sigma_{\rm syst} = +1$: $\mathscr{L}_0(E > 10^{17}\ {\rm eV}) = 2.4 \cdot 10^{46}\ {\rm erg\ Mpc^{-3}\ yr^{-1}}$ $\mathscr{L}_0(E > 10^{17}\ {\rm eV}) = 5.6 \cdot 10^{44}\ {\rm erg\ Mpc^{-3}\ yr^{-1}}$

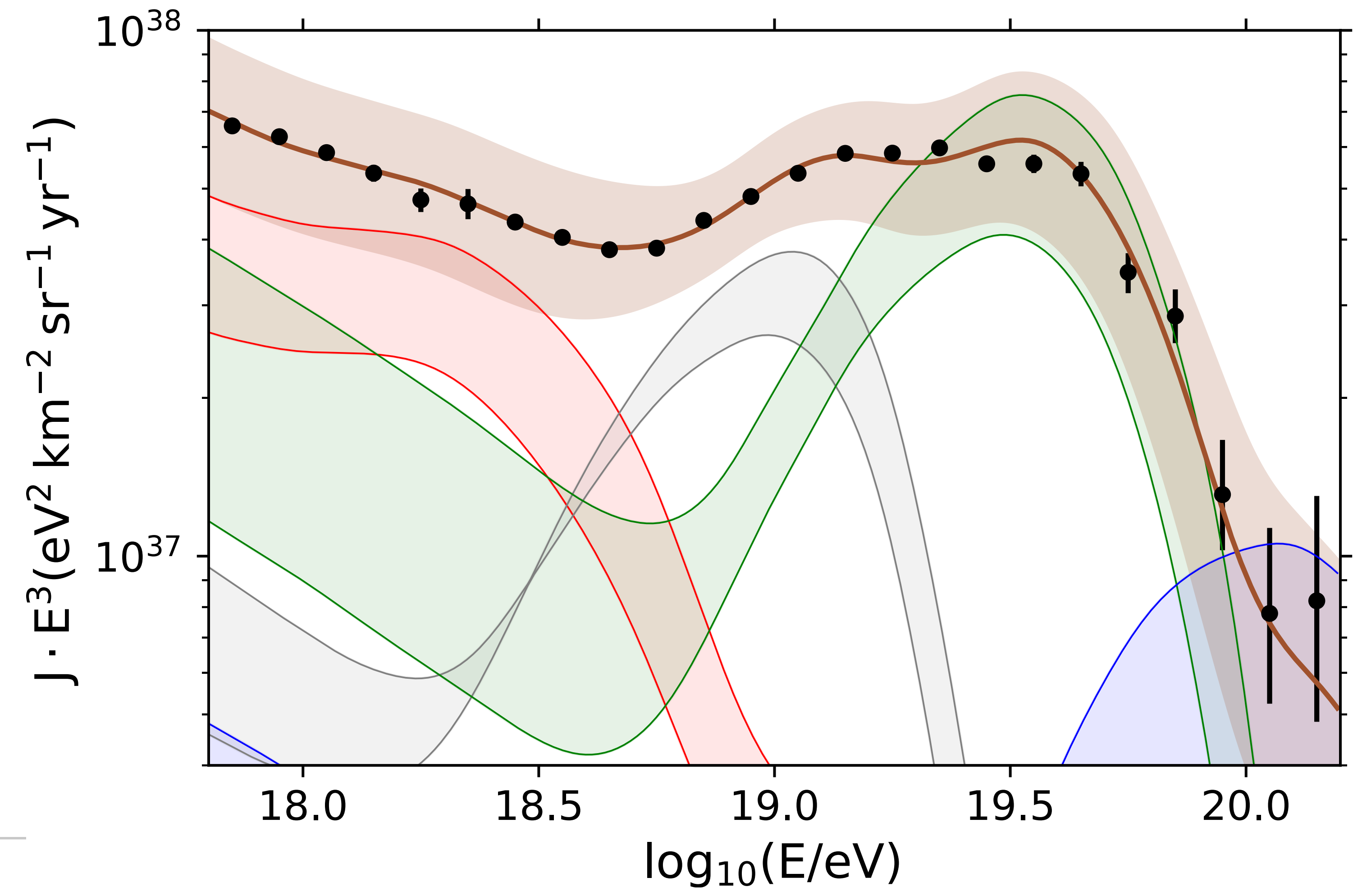

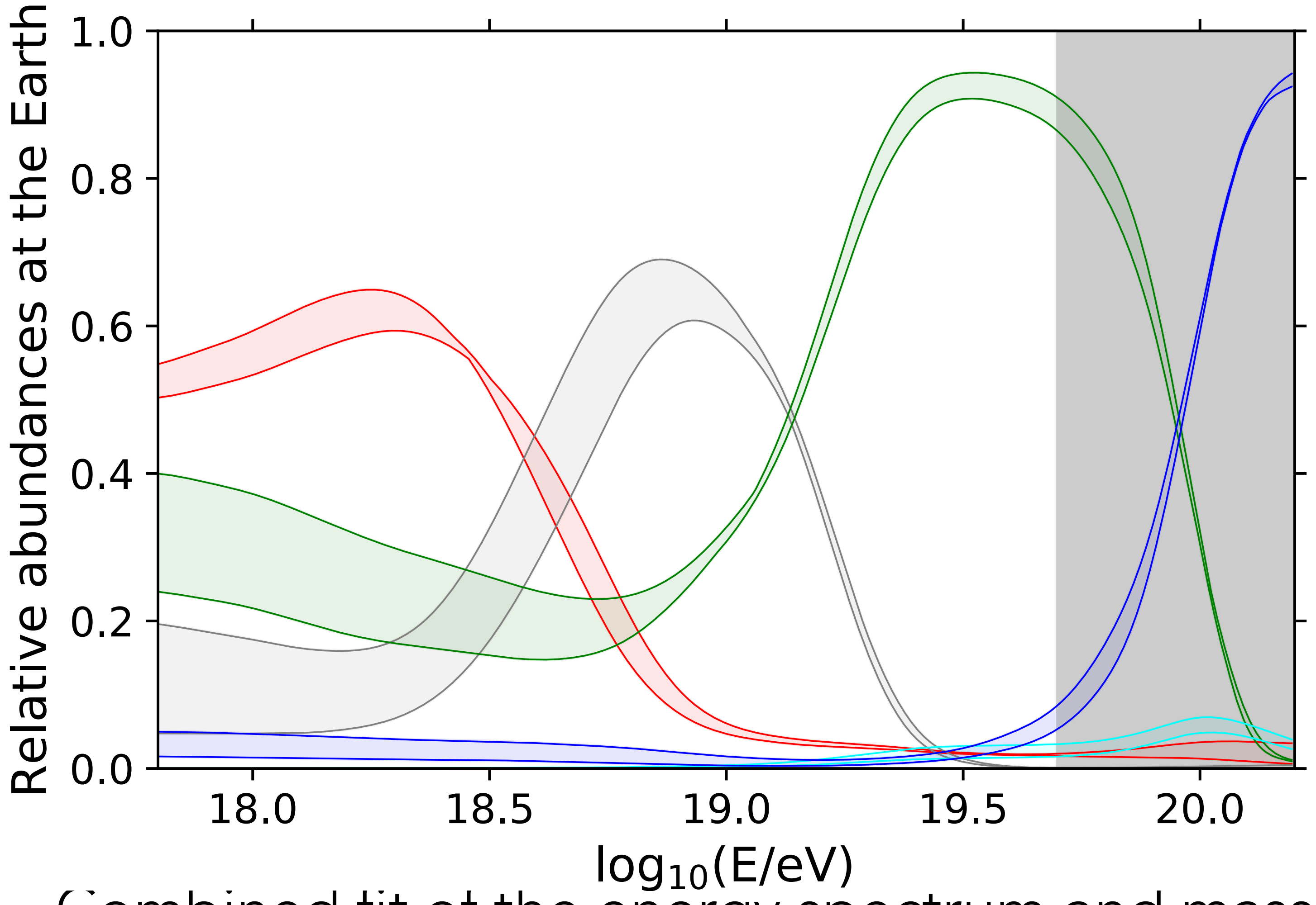

Effect of the systematic uncertainties

Systematic uncertainties from models:

<u>Hadronic interaction model:</u> Sibyll2.3d / EPOS-LHC / intermediate models

- If δ_{HIM} is close to 1 → EPOS-LHC is dominant
- If δ_{HIM} is close to 0 → Sibyll2.3d is dominant

<u>Propagation model effect:</u>

fit repeated considering different model configurations

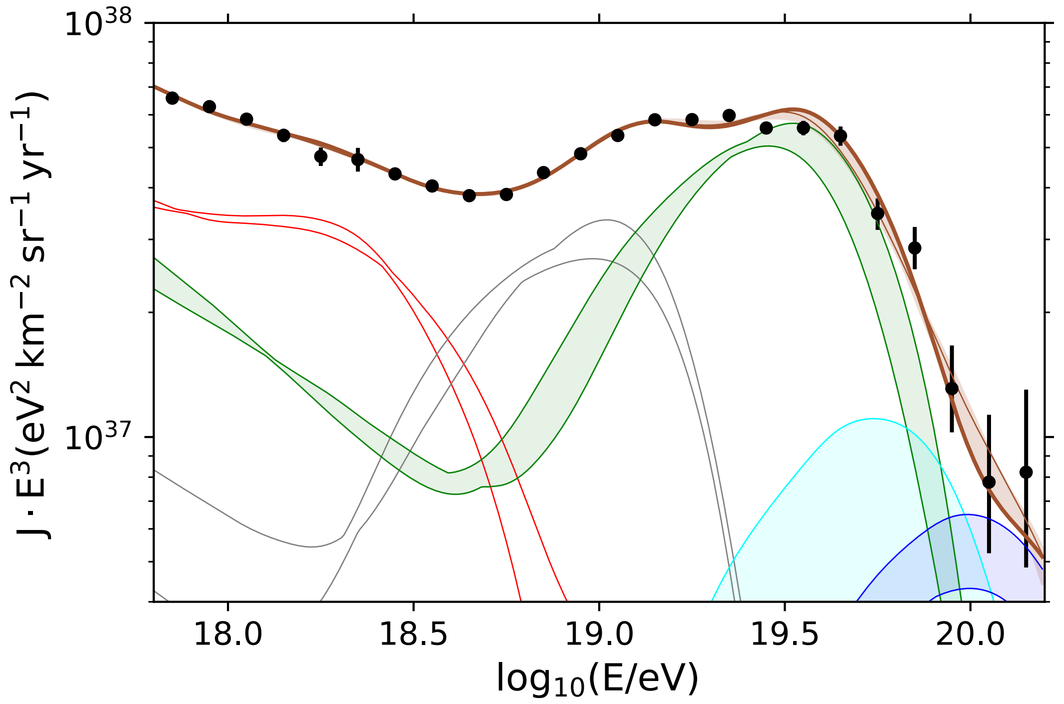

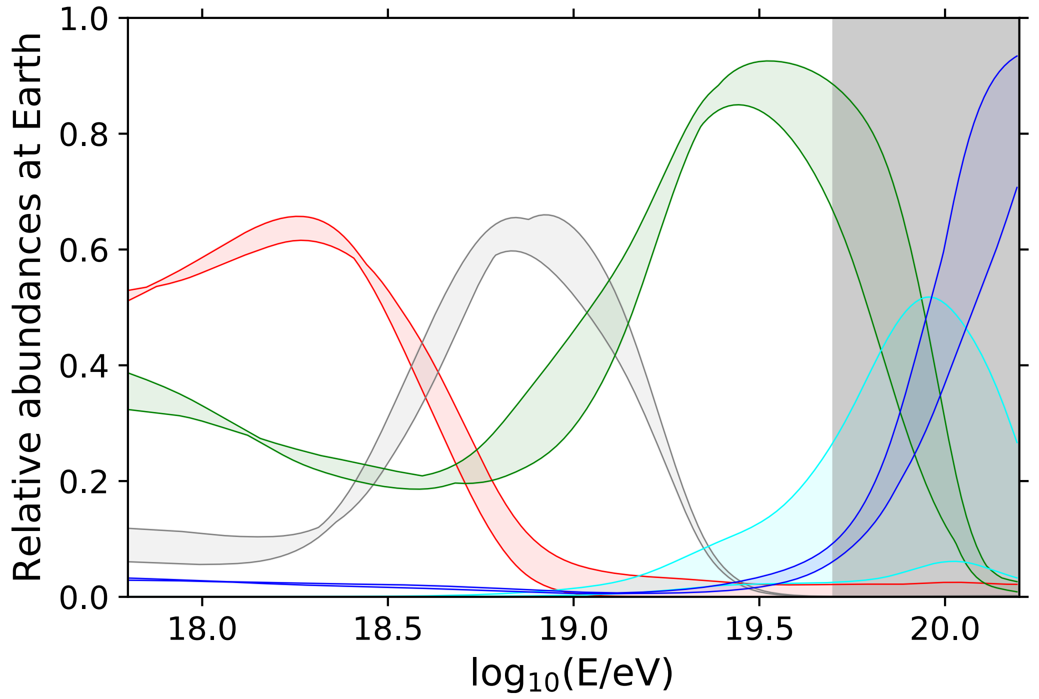

	Talys, Gilmore		PSB, Gilmore		Talys, Dominguez		PSB, Dominguez	
	LE	HE	LE	HE	LE	HE	LE	HE
$\mathcal{L}_0$ $[10^{45}\mathrm{erg\ Mpc^{-3}yr^{-1}}]$	17.0	0.45	16.8	0.44	21.7	0.71	22.1	0.71
γ	3.49 ± 0.02	-1.98 ± 0.10	3.49 ± 0.03	-1.95 ± 0.16	3.67 ± 0.06	-0.95 ± 0.12	3.70 ± 0.05	-0.94 ± 0.12
$\log_{10}(R_{\mathrm{cut}}/\mathrm{V})$	24 (lim.)	18.16 ± 0.01	24 (lim.)	18.16 ± 0.02	18.04 ± 0.06	18.23 ± 0.02	18.03 ± 0.02	18.22 ± 0.02
I_{H} (%)	49.87	0.0	51.15	0.91	45.48	0.61	45.67	0.79
I_{He} (%)	10.92	28.60	12.68	49.09	6.13	20.25	8.55	48.79
I_{N} (%)	36.25	69.05	33.25	43.89	45.03	73.70	42.10	40.57
I_{Si} (%)	0.0	7.32	0.0	4.23	0.0	2.75	0.0	7.99
I_{Fe} (%)	2.96	2.35	2.93	1.87	3.36	2.69	3.67	1.86
δ_{HIM}	1.0 (lim.)		1.0 (lim.)		$0.96^{+0.04}_{-0.16}$		$0.94^{+0.06}_{-0.14}$	
D_J (N_J)	60.1 (24)		53.0 (24)		44.7 (24)		43.0 (24)	
$D_{X_{\max}}$ $(N_{X_{\max}})$	554.8 (329)		562.8 (329)		586.3 (329)		591.6 (329)	
D (N)	614.9 (353)		615.8 (353)		631.0 (353)		634.6 (353)	

- *<u>EPOS-LHC or models compatible with it are always preferred</u>*

  → **HIM choice: stronger impact on D and on the predictions at Earth**

- *Propagation models*: some expected changes in the best fit parameters

Effect of the systematic uncertainties

	Talys, Gilmore		PSB, Gilmore		Talys, Dominguez		PSB, Dominguez	
	LE	HE	LE	HE	LE	HE	LE	HE
$\mathcal{L}_0$ $[10^{45}\text{erg Mpc}^{-3}\text{yr}^{-1}]$	17.0	0.45	16.8	0.44	21.7	0.71	22.1	0.71
γ	3.49 ± 0.02	-1.98 ± 0.10	3.49 ± 0.03	-1.95 ± 0.16	3.67 ± 0.06	-0.95 ± 0.12	3.70 ± 0.05	-0.94 ± 0.12
$\log_{10}(R_\text{cut}/\text{V})$	24 (lim.)	18.16 ± 0.01	24 (lim.)	18.16 ± 0.02	18.04 ± 0.06	18.23 ± 0.02	18.03 ± 0.02	18.22 ± 0.02
I_H (%)	49.87	0.0	51.15	0.91	45.48	0.61	45.67	0.79
I_He (%)	10.92	28.60	12.68	49.09	6.13	20.25	8.55	48.79
I_N (%)	36.25	69.05	33.25	43.89	45.03	73.70	42.10	40.57
I_Si (%)	0.0	7.32	0.0	4.23	0.0	2.75	0.0	7.99
I_Fe (%)	2.96	2.35	2.93	1.87	3.36	2.69	3.67	1.86
δ_HIM	1.0 (lim.)		1.0 (lim.)		$0.96^{+0.04}_{-0.16}$		$0.94^{+0.06}_{-0.14}$	
D_J (N_J)	60.1 (24)		53.0 (24)		44.7 (24)		43.0 (24)	
D_{X_max} (N_{X_max})	554.8 (329)		562.8 (329)		586.3 (329)		591.6 (329)	
D (N)	614.9 (353)		615.8 (353)		631.0 (353)		634.6 (353)	

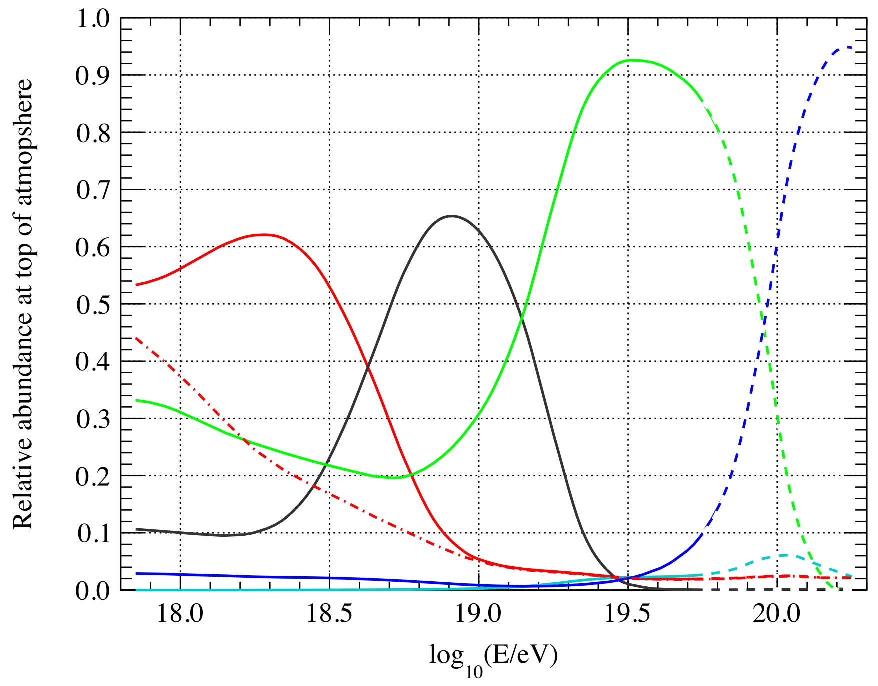

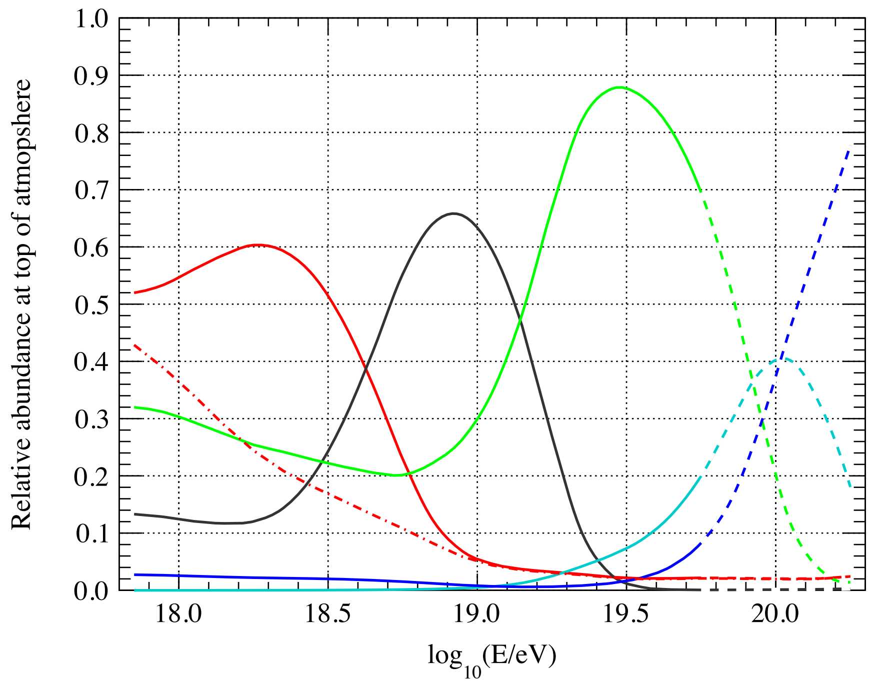

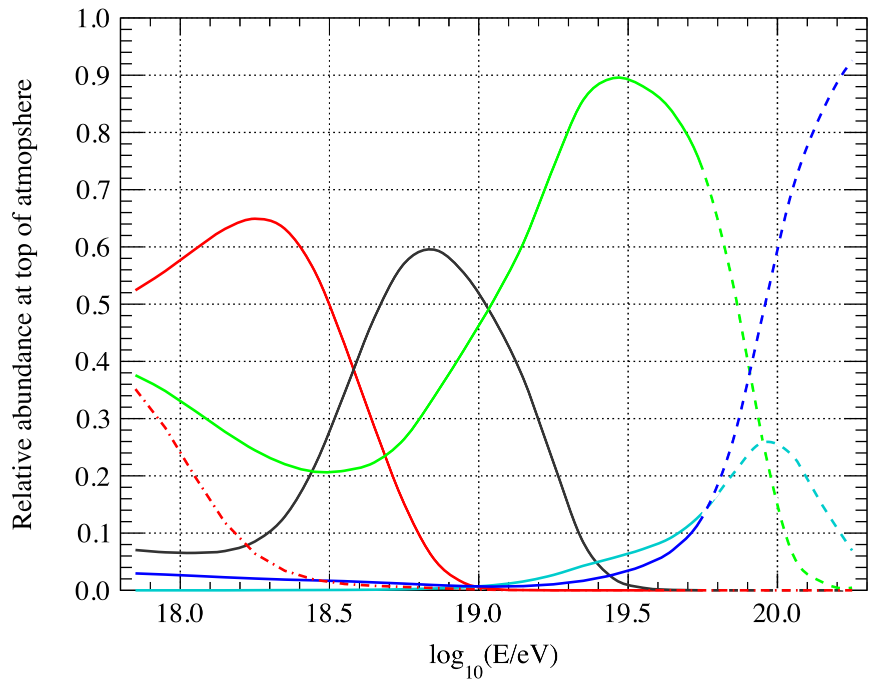

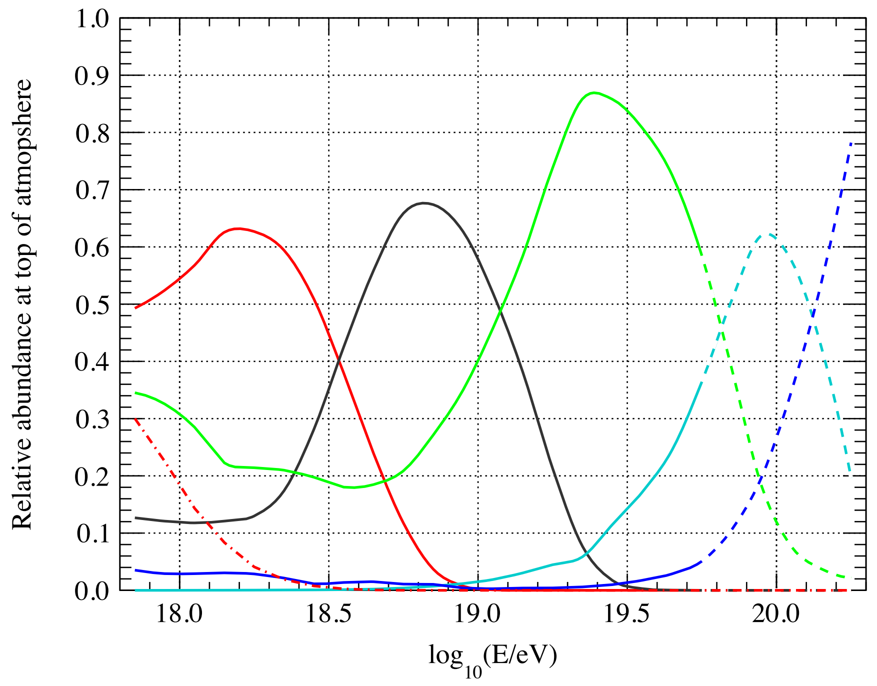

The energy density integral fractions

- Mass fractions defined at $E_0 <$ the fit threshold → strong dependence on γ

  → not really informative about the mass composition at the sources

$$\rightarrow \quad I_A = \frac{\int_{E_{\min}}^{\infty} J_A(E) E dE}{\sum_A \int_{E_{\min}}^{\infty} J_A(E) E dE}$$

Fractions of the integral of the energy density above $E_{min} = 10^{17}$ eV

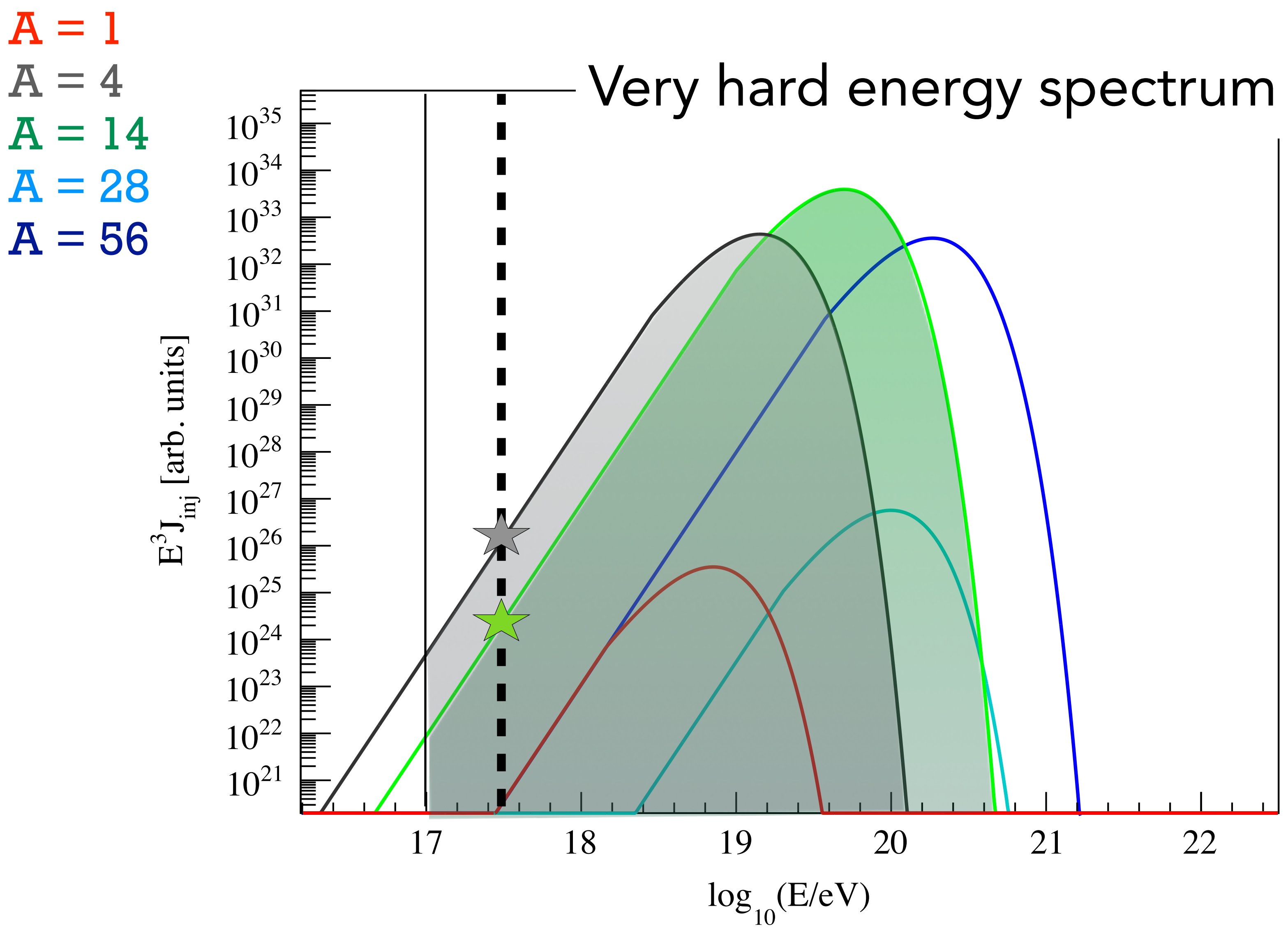

f_H (%)	O(10^{-4})
f_{He} (%)	98
f_N (%)	2
f_{Si} (%)	O(10^{-9})
f_{Fe} (%)	O(10^{-4})

→

I_H (%)	O(10^{-6})
I_{He} (%)	28
I_N (%)	70
I_{Si} (%)	O(10^{-6})
I_{Fe} (%)	2

- Emissivity of a population: total energy ejected per unit of comoving volume and time

at $z = 0$: $\mathscr{L}_0 = \sum_A \int_{E_{\min}}^{\infty} E\, q_A(E)\, dE$

expressed in $\mathrm{erg} \cdot \mathrm{Mpc}^{-3} \cdot \mathrm{yr}^{-1}$

$q_A(E) \propto J_A(E) \cdot 4\pi / r(z_{\max})$

expressed in $\mathrm{erg}^{-1} \cdot \mathrm{Mpc}^{-3} \cdot \mathrm{yr}^{-1}$

Systematic uncertainties in JCAP2017 (above-ankle fit)

$\Delta X_{\max}$	$\Delta E/E$	γ	$\log_{10}(R_{\rm cut}/{\rm V})$	D	$D(J)$	$D(X_{\max})$
	-14%	$+1.33\pm0.05$	18.70 ± 0.03	167.0	19.0	148.0
$-1\sigma_{\rm syst}$	0	$+1.36\pm0.05$	$18.74^{+0.03}_{-0.04}$	166.7	14.7	152.0
	$+14\%$	$+1.39^{+0.03}_{-0.05}$	$18.79^{+0.03}_{-0.04}$	169.6	13.0	156.6
	-14%	$+0.92^{+0.09}_{-0.10}$	18.65 ± 0.02	176.1	18.1	158.0
0	0	$+0.96^{+0.08}_{-0.13}$	$18.68^{+0.02}_{-0.04}$	174.3	13.2	161.1
	$+14\%$	$+0.99^{+0.08}_{-0.12}$	$18.71^{+0.03}_{-0.04}$	176.3	11.7	164.4
	-14%	$-1.50^{+0.08}_{*}$	18.22 ± 0.01	208.1	15.3	192.8
$+1\sigma_{\rm syst}$	0	$-1.49^{+0.16}_{*}$	$18.25^{+0.02}_{-0.01}$	202.6	9.7	192.8
	$+14\%$	$-1.02^{+0.37}_{-0.44}$	18.35 ± 0.05	206.4	11.3	195.1

*This interval extends all the way down to -1.5, the lowest value of γ we considered.

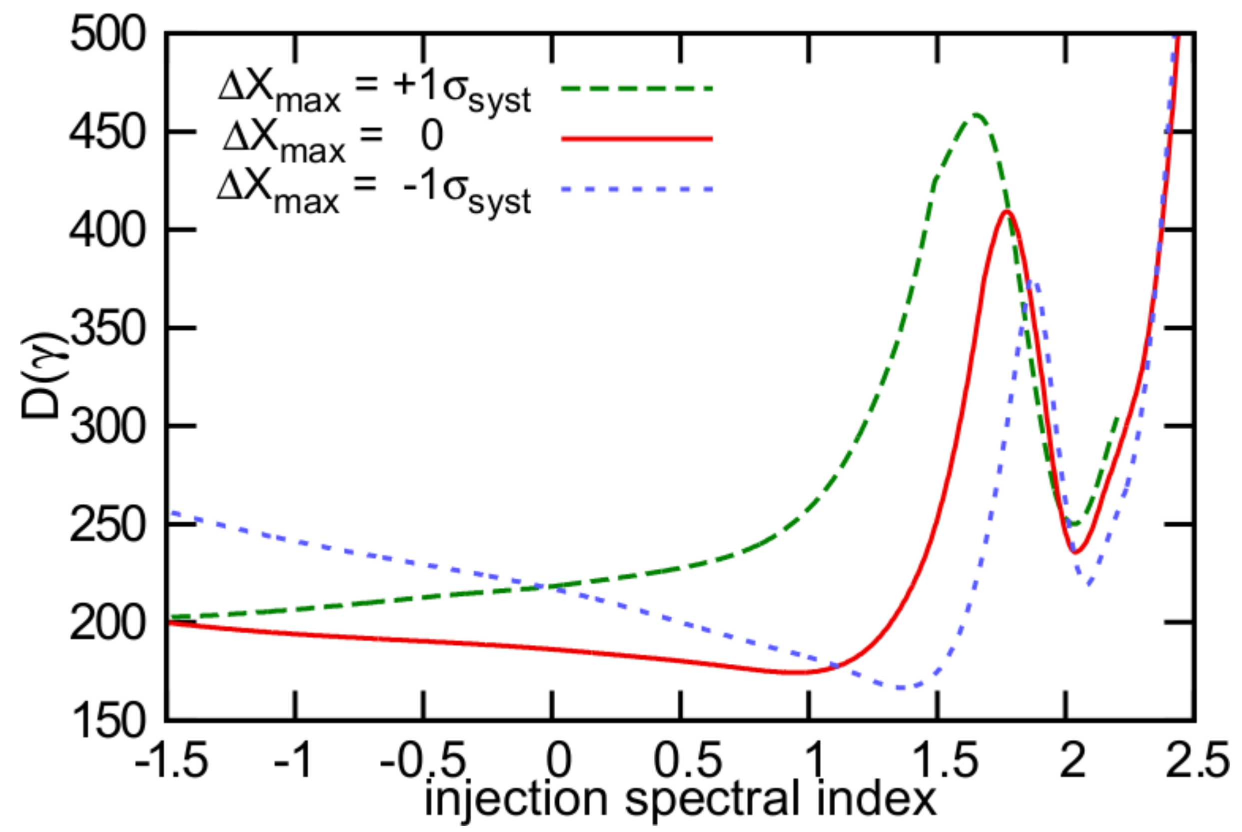

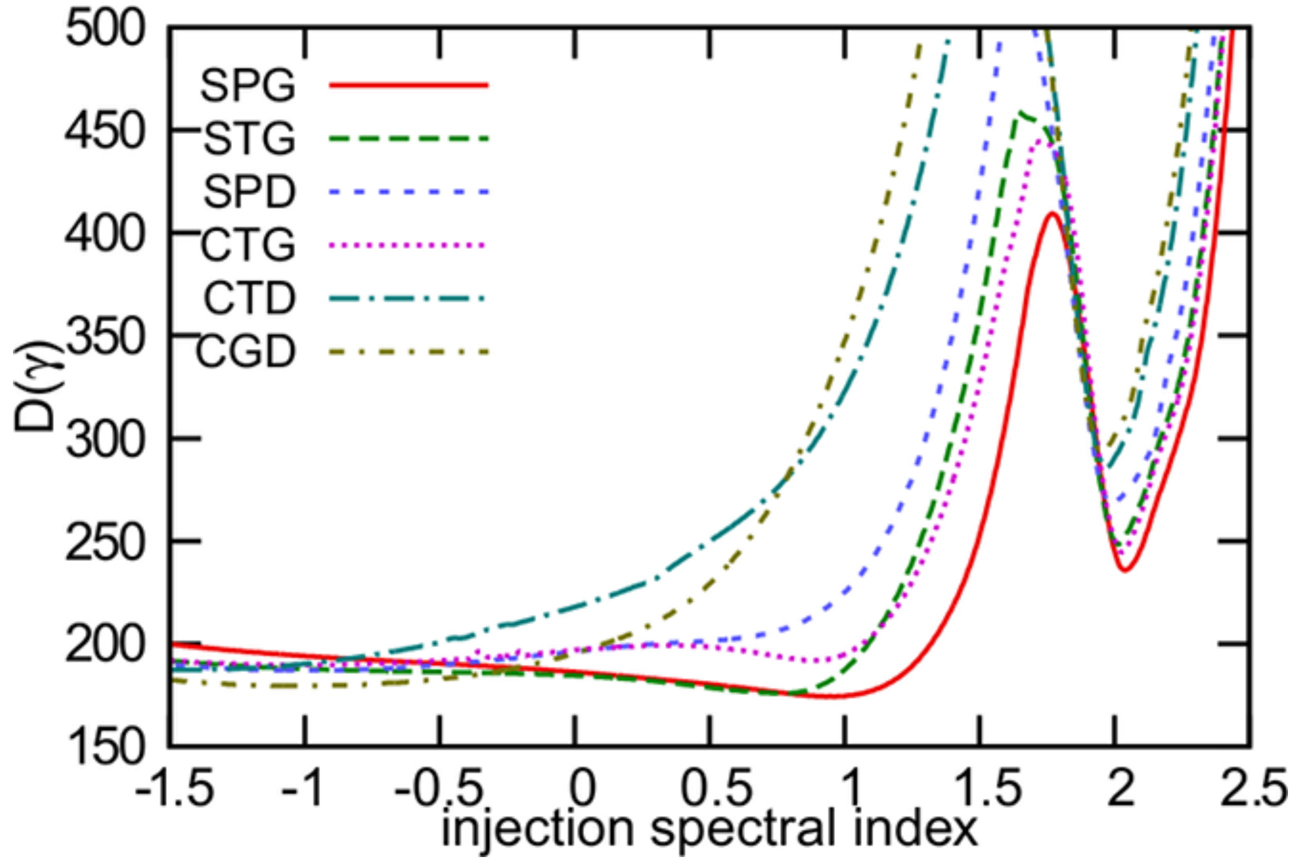

From JCAP2017

Systematic uncertainties from models (above-ankle fit)

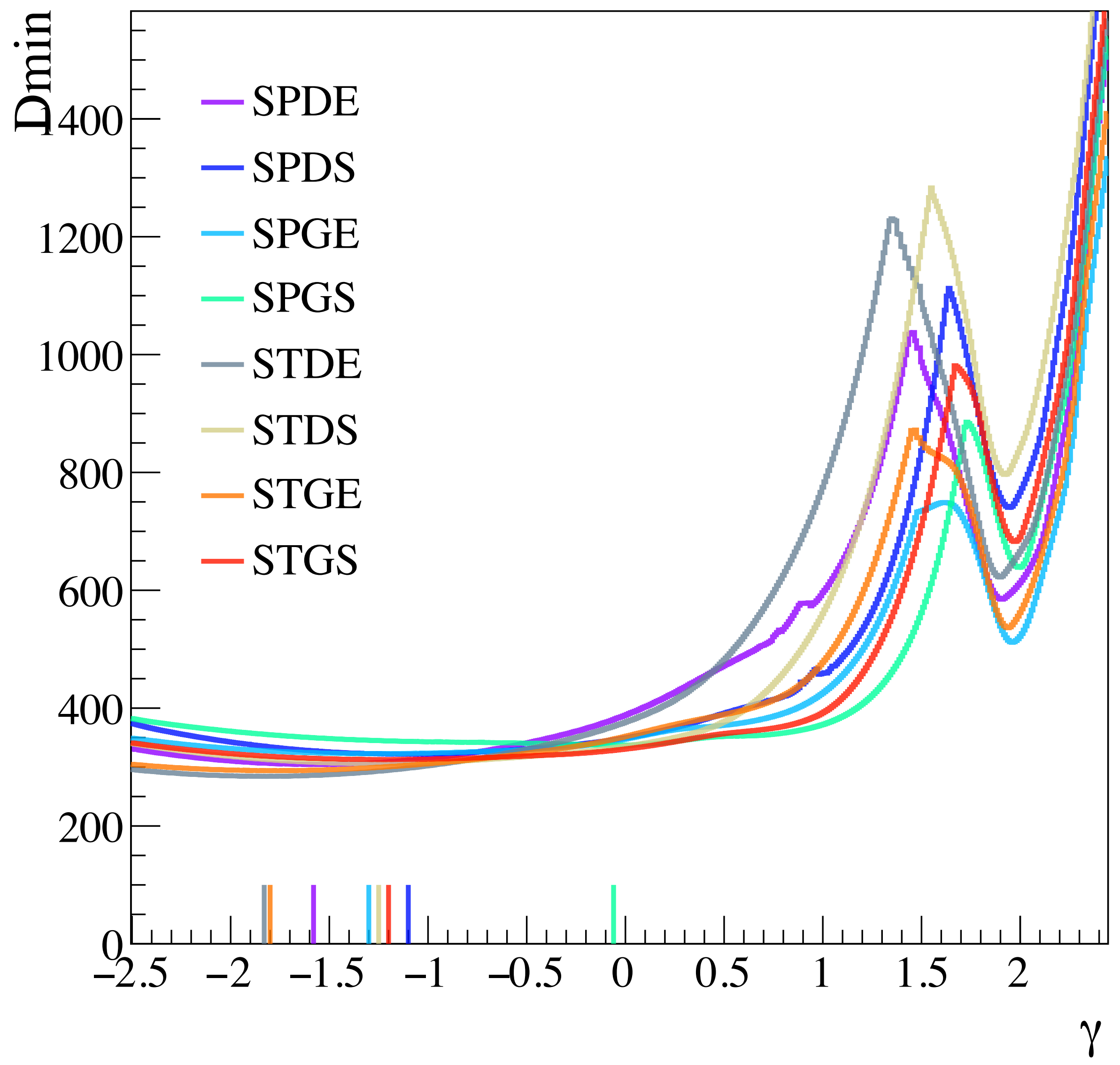

- Effect of the systematic uncertainties from models in the above-ankle fit
- For negative spectral indices the deviance is almost flat
- The statistical uncertainties are very small so that each configuration has a different minimum, generally not compatible with the others within the D_{min}+1 interval

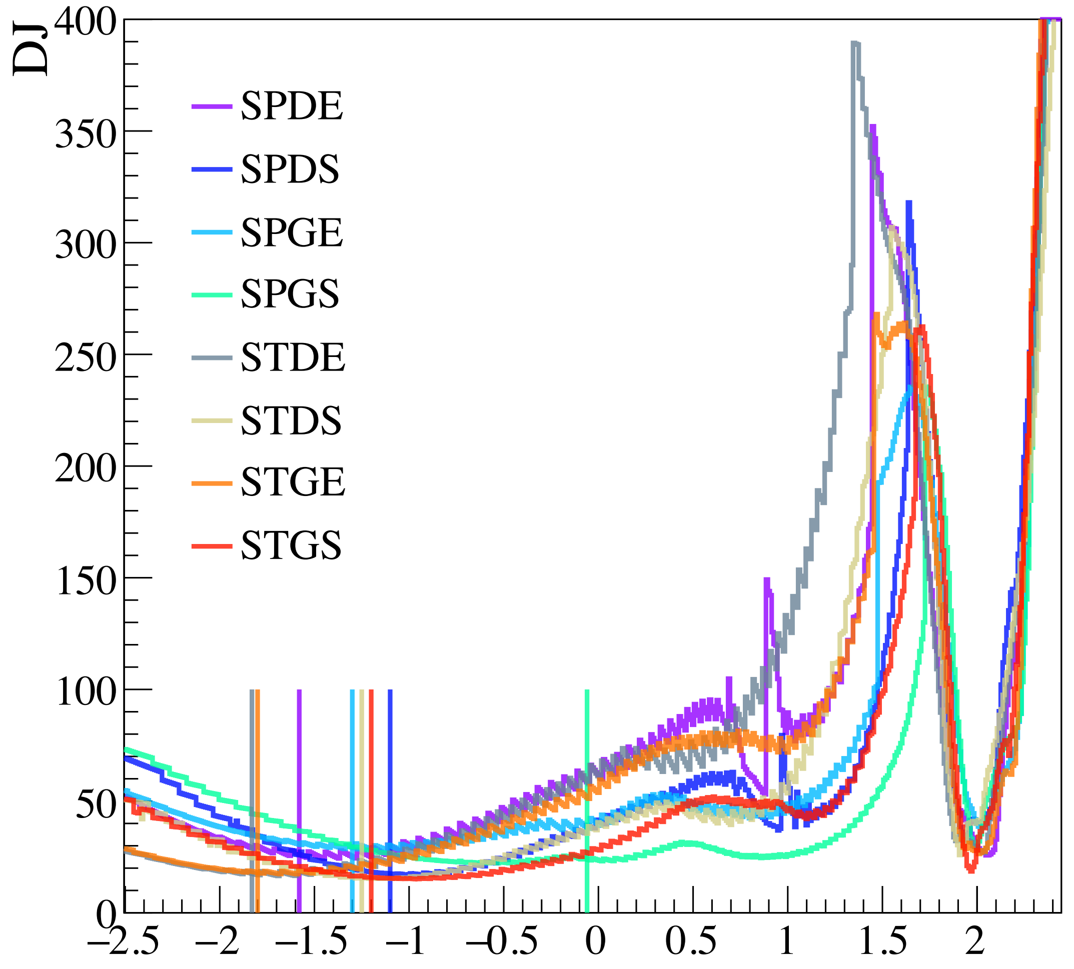

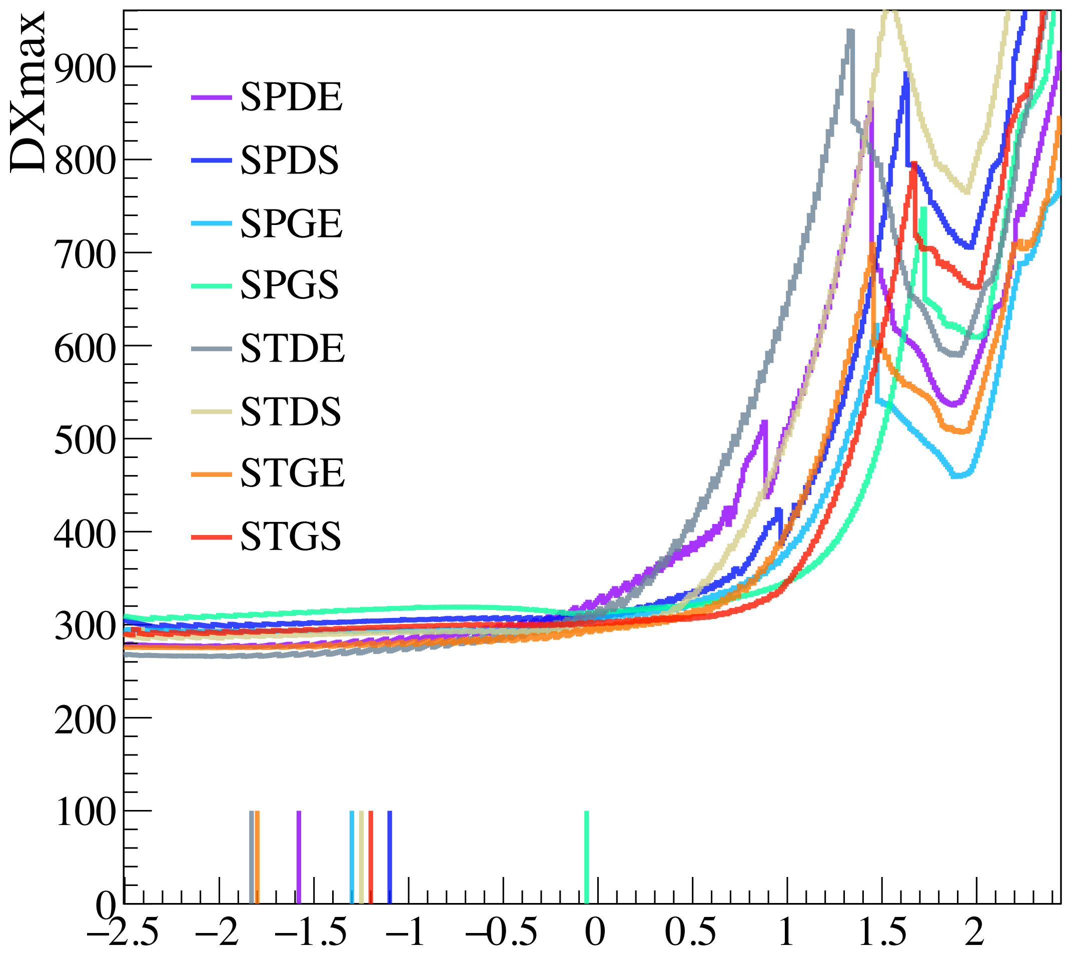

Plots from S. Petrera

Mean rigidity vs energy

Loop over the energy bins

$f_A(A, \log(E))$ is the fraction of nuclei A at energy E (from the fit)

For each possible mass number A at the Earth (A from 1 to 56):

$A \rightarrow Z(A)$ (atomic number for a stable nucleus with mass number A)

Mean atomic number <Z> at energy E : $< Z > (\log(E)) = \Sigma_A \; f_A(A, \log(E)) \cdot Z(A)$

The mean rigidity is : $< R > = \Sigma_A \; f_A(A, \log(E)) \cdot E/Z(A)$

$$< \log R > = \Sigma_A \; f_A(A, \log(E)) \cdot (\log(E) - \log(Z(A)))$$

Mean rigidity vs energy

	Talys, Gilmore		PSB, Gilmore		Talys, Dominguez		PSB, Dominguez	
	LE	HE	LE	HE	LE	HE	LE	HE
$\mathcal{L}_0$ [10^{45}erg Mpc^{-3}yr^{-1}]	17.0	0.45	16.8	0.44	21.7	0.71	22.1	0.71
γ	3.49 ± 0.02	-1.98 ± 0.10	3.49 ± 0.03	-1.95 ± 0.16	3.67 ± 0.06	-0.95 ± 0.12	3.70 ± 0.05	-0.94 ± 0.12
$\log_{10}(R_{\rm cut}/{\rm V})$	24 (lim.)	18.16 ± 0.01	24 (lim.)	18.16 ± 0.02	18.04 ± 0.06	18.23 ± 0.02	18.03 ± 0.02	18.22 ± 0.02
$I_{\rm H}$ (%)	49.87	0.0	51.15	0.91	45.48	0.61	45.67	0.79
$I_{\rm He}$ (%)	10.92	28.60	12.68	49.09	6.13	20.25	8.55	48.79
$I_{\rm N}$ (%)	36.25	69.05	33.25	43.89	45.03	73.70	42.10	40.57
$I_{\rm Si}$ (%)	0.0	7.32	0.0	4.23	0.0	2.75	0.0	7.99
$I_{\rm Fe}$ (%)	2.96	2.35	2.93	1.87	3.36	2.69	3.67	1.86
$\delta_{\rm HIM}$	1.0 (lim.)		1.0 (lim.)		$0.96^{+0.04}_{-0.16}$		$0.94^{+0.06}_{-0.14}$	
D_J (N_J)	60.1 (24)		53.0 (24)		44.7 (24)		43.0 (24)	
$D_{X_{\rm max}}$ ($N_{X_{\rm max}}$)	554.8 (329)		562.8 (329)		586.3 (329)		591.6 (329)	
D (N)	614.9 (353)		615.8 (353)		631.0 (353)		634.6 (353)